

Neograd: Gradient Descent with a Near-Ideal Learning Rate

Michael F. Zimmer

ZIM@NEOMATH.COM

Abstract

Since its inception by Cauchy in 1847, the gradient descent algorithm has been without guidance as to how to efficiently set the learning rate. This paper identifies a concept, defines metrics, and introduces algorithms to provide such guidance. The result is a family of algorithms (Neograd) based on a *constant ρ ansatz*, where ρ is a metric based on the error of the updates. This allows one to adjust the learning rate at each step, using a formulaic estimate based on ρ . It is now no longer necessary to do trial runs beforehand to estimate a single learning rate for an entire optimization run. The additional costs to operate this metric are trivial. One member of this family of algorithms, NeogradM, can quickly reach much lower cost function values than other first order algorithms. Comparisons are made mainly between NeogradM and Adam on an array of test functions and on a neural network model for identifying hand-written digits. The results show great performance improvements with NeogradM.

Keywords: Gradient descent, learning rate, Adam, Neograd, rho

1. Introduction

Gradient descent (GD) is an iterative optimization method, designed to find the minimum of a specified cost function (CF). The method has found diverse applications across numerous fields since it was discovered by Cauchy (1847). In particular, it finds frequent use in the field of machine learning (ML), and the lack of a robust and efficiently adaptive learning rate for the method has been a long-lived impediment in its application. The GD algorithm operates by searching the parameter space over which the function is defined, starting from some initial value. The updates to this starting parameter value are proportional to the product of the gradient of the function and a scalar (the *learning rate*). While this is a straightforward and fairly stable method, it is challenged by certain types of CFs. It is the purpose of this paper to explain a new method to control the learning rate, so the GD method is (almost) never overly challenged by such CFs. Also, when used in the context of ML, it is highlighted that this paper primarily addresses the use of GD with *batch* processing, as opposed to mini-batch or stochastic gradient descent (Goodfellow et al., 2016).

This paper begins with the section "Gradient descent" reviewing the most basic form of GD. It is followed by sub-sections on certain extant variations of GD, considerations on an ideal GD method, and finally a new derivation of GD. The next section "Measures of control", introduces the concept of "Update Fidelity" and three diagnostic metrics (ρ , dotp, sumd) which are meant to inform the user of the progress of the algorithm. In particular, the ρ (ρ) diagnostic will be seen to form the basis for a new family of algorithms. Next, in the section "Computing ρ ", a convenient means of computing ρ for batch GD is introduced, which involves almost no additional cost over the usual approach. In the following section, "Solutions for simple cases", an examination is made of the role and use of ρ in GD when the CF is one of several simple forms; these forms include a quadratic, a quartic, an ellipse, and a simple well formed from two sigmoids. The purpose of this is to help build intuition about ρ , as this is a new metric. The next section, "Algorithms", begins with two sub-sections on the theoretical basis for adaptively updating the learning rate. The sub-sections

that follow contain pseudocode for the algorithms that comprise the Neograd family. The following section, "Experiments", contains selected comparisons and analyses of this family of algorithms. Each experiment was chosen to demonstrate at least one particular point or feature. For the most part, this section uses special functions, but it also includes a neural net model to recognize handwritten digits. The last section, "Final Remarks", contains a summary, comparison and perspective. Two appendices are also included: one providing background on the linear algebra solution used for the new derivation of GD, and another discussing an alternative definition of ρ . Accompanying code for this paper can be found elsewhere (Zimmer, 2020b).

2. Gradient Descent (GD)

The GD algorithm (Press et al., 2007) is an iterative method for finding the minimum of a C^1 function f . With f defined over θ , the algorithm begins with the initial choice of θ_0 , and defines updates according to the formula

$$\theta = \theta_0 - \alpha \nabla f|_{\theta_0},$$

where α is a small positive constant known as the *learning rate*. This update step, along with a re-evaluation of f and ∇f , is repeated until a suitable stopping condition is met. This algorithm is motivated by the fact that the gradient of a function points in the direction of its maximal increase, and so its negative must point toward its maximal decrease.

This would appear to be a straightforward, perhaps even robust approach to determining the minimum, and one should only have the trivial task of setting α to some suitably small number. However, even for simple functions such as $f = \theta^4$, it can be shown (cf. Section 5.2) that any value of α will lead to unstable behavior for a sufficiently large θ_0 . When this trivial quartic function is replaced by the much more complex CFs used in ML applications, the situation becomes exponentially compounded.

2.1 Existing Variations on Gradient Descent

This section does not attempt to compare and contrast all the existing GD variations that are known (cf. Ruder, 2017), here called the "GD family". Instead, the purpose is to mention two prominent themes that appear in some of the more widely used algorithms. The first such theme is momentum (Polyak, 1964), which instead of using the current gradient utilizes an exponentially weighted average of past gradients (weighted in favor of the more recent updates). While this can be useful in smoothing over zig-zagging updates, it can be detrimental if the momentum parameter is set too large since it may cause the updates to adjust too slowly. A variation on this is Nesterov momentum Nesterov (1983), which uses a look-ahead approach toward computing the momentum, and hence acquires some second-order capabilities.

The second theme is a sort of "preferential weighting", and uses heuristics to re-weight the update from basic GD. For this category, the approaches of AdaGrad (Duchi et al., 2011), AdaDelta (Zeiler, 2012), RMS Prop (Tieleman and Hinton, 2012), Adam (Kingma and Ba, 2015) and others (see Ruder, 2017) may be grouped together. The heuristic represented by this group is basically that gradients that are small should contribute more, and those that are large should contribute less. In doing this it is hoped that the problems mentioned previously (zig-zagging, flat/steep CF) will be ameliorated. Also, note that these two themes can overlap, such as with Adam, producing an algorithm that incorporates momentum and a preferential weighting scheme.

There are other approaches that aren't easily classified into one of these two schemes. Among them is the line search method (Press et al., 2007), which tries several values of the learning rate and selects the one yielding the lowest CF. Also, the whole class of second-order methods will not be considered here, as it's outside the scope of this paper. As a general comment though, those methods tend to yield improved results, but at a higher computational cost. Finally, there are a number of heuristics, both with respect to learning rate schedules (e.g., " $1/t$ " decay, Li et al., 2020) and other modified gradients (e.g., norm clipping, Pascanu et al., 2013). Keep in mind, the comparisons here are only for straight optimization (i.e., batch training), and some of these methods perform best for mini-batch training. For example, the " $1/t$ " decay would have $\alpha \propto 1/t$, but it will be shown on a certain example the best results occur when α increases to *large* values. For these reasons comparisons will not be made to these approaches.

2.2 An Ideal Gradient Descent Algorithm

An ideal variation of the basic GD algorithm will gracefully handle any challenge that may appear. To be sure, these challenges arise from the landscape of the CF, which may have one or many minima and potentially many saddle points, as well as narrow valleys, steep cliffs, and nearly flat regions. The narrow valleys tend to lead to oscillating behavior in the updates (Press et al., 2007); the flat regions may lead to a vanishing gradient, and the cliffs lead to exploding gradients (Pascanu et al., 2013).

An important concept here is the *basin of attraction*, which is just the region of parameter space defined by all the initial θ values that eventually lead to a small neighborhood of the same minimum, after doing a sufficient number of arbitrarily small updates. If the value of α is set so large that updates lead it to frequently leave its basin of attraction then it is essentially no longer acting as a GD algorithm. Instead, it is perhaps more like a simple random sampling algorithm.

The approach that's normally taken is to attempt to find a "best" learning rate (α). This is done by doing a number of optimization runs with different values of α , and comparing the plots of: training cost vs. iterations. However, even the idea of finding a single, best α is flawed. By analogy, it's equivalent to trying to find the "best speed" at which to drive between two distant cities. For example, to drive from Chicago to St Louis, would the best speed be 10mph, 50mph, or 100mph? As with optimization, a higher rate does not always lead to a better outcome. Since a single α does not seem to suffice, this paper will pursue a different route: an adaptive algorithm for α , one that can navigate between the Scylla and Charybdis of high and low learning rates.

Another issue is the judging of optimization algorithms by how well the resulting ML model *generalizes*. While generalization is the ultimate goal of creating an ML model, it largely consists of optimization *plus* regularization. The focus here is solely on optimization; the ability to generalize will be ignored.

2.3 Another Derivation of Gradient Descent

This section is provided to not only give a new derivation of the GD algorithm, but to do so in a way that provides insight into the relationship between basic GD and some of its variations (i.e., momentum, preferential weighting). Begin with a Taylor series expansion of the cost function f

$$f(\theta) = f(\theta_0) + \nabla f|_{\theta_0} \cdot d\theta + \dots,$$

where $d\boldsymbol{\theta} = \boldsymbol{\theta} - \boldsymbol{\theta}_0$. What is sought is a decrease in f , so that $\delta f = f(\boldsymbol{\theta}) - f(\boldsymbol{\theta}_0)$ is negative. To make the sign explicit, it is replaced with $-|\delta f|$. Thus a first-order solution for $d\boldsymbol{\theta}$ is sought for this equation:

$$\nabla f(d\boldsymbol{\theta})^T = -|\delta f|. \tag{1}$$

It can be interpreted as a system of linear equations $Ax = b$, where $A = \nabla f$, $x = (d\boldsymbol{\theta})^T$, and $b = -|\delta f|$. If $\boldsymbol{\theta}$ is n -dimensional, A is a 1-by- n matrix, x is an n -dimensional column vector, and b is a scalar. So long as $n > 1$, this is an under-determined system of equations, and the inverse A^{-1} will not exist. Nevertheless, it's possible to instead formulate the solution using a generalized inverse. A new technique (Zimmer, 2020c) for solving it in this manner is given in Appendix A. It is based on the row space of A and yields the solution

$$d\boldsymbol{\theta} = \frac{(\nabla f)^T}{\|\nabla f\|^2}(-|\delta f|) + d\boldsymbol{\theta}_{null},$$

where the first term on the right-hand side is the particular solution, and the second term is the homogeneous (or null space) solution. After identifying the learning rate as $\alpha = |\delta f|/\|\nabla f\|^2$, which is a positive constant, the final form for the update of $\boldsymbol{\theta}$ is

$$d\boldsymbol{\theta} = -\alpha(\nabla f)^T + d\boldsymbol{\theta}_{null}. \tag{2}$$

This solution becomes a minimum-norm solution when $\|d\boldsymbol{\theta}_{null}\| = 0$. This means that for the updates to make the quickest descent possible, it should use $d\boldsymbol{\theta} = -\alpha(\nabla f)^T$, which is just the usual GD. Observe that when momentum or preferential weighting is used, $d\boldsymbol{\theta}_{null} \neq 0$; this contribution to the solution is *perpendicular* to the gradient. It leads to an update partially following the level-set contours of constant f , as opposed to the direction dictated by a pure GD.

3. Measures of Control

"Measure what is measurable, and make measurable what is not so." (Cournot and Martin)

Toward achieving the goal of a GD algorithm with an adaptive learning rate, a concept and several diagnostic metrics are introduced. As will be seen, the most important is the *rho* (ρ) diagnostic, which gives a measure of whether α is too large or small. Also, the *dotp* diagnostic informs the decision on the target value used for ρ , and the *sumd* diagnostic informs the decision on whether a stopping condition has been met.

3.1 Update Fidelity (UF)

This section puts a name on something probably everyone who has worked with GD has understood at some level. It is that it's possible to choose the learning rate α to be too large or too small, and in either case the result will be suboptimal; the best choice lies somewhere in between. Here that situation is illustrated in Fig. 1 with three plots of GD updates done on a quadratic CF, with each one having a different α . In each figure the initial point is marked with a red dot. A GD update is made, and its prediction for the new CF value is indicated by the end of a straight (red) line. The new (actual) CF value is marked with another red dot on the CF; from there, another GD update is

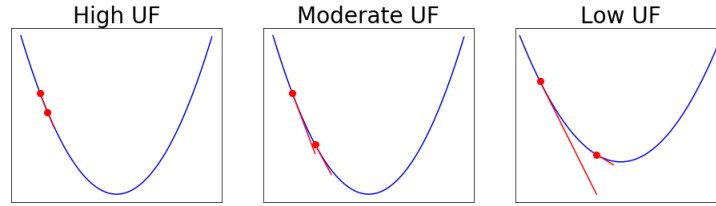


Figure 1: Illustration of UF using GD on $f = \theta^2$ with $\alpha = 0.05, 0.15, 0.35$ for high, moderate and low UF, respectively. Update fidelity is exhibited by the degree to which the red lines (i.e., the GD updates) overlap f .

made, and another line drawn. It's important to remember that GD is a linear extrapolation in α for both $d\theta$ and f . The three figures, from left to right, have increasing values of α , which correspond to decreasing UF. Thus, the UF is "figuratively understood" to be the degree to which these linear extensions/predictions coincide with the underlying curve.

With that in mind, what these three figures indicate is that with high UF, the linear updates/predictions (i.e., red lines) are close to the underlying function, and it makes slow progress toward the minimum of the function. For low UF, the linear updates/predictions differ significantly from the underlying function, and perhaps can't be trusted to lead to stable behavior during optimization. In contrast to these two extremes, the case of a moderate UF represents a compromise that the user of GD aims to achieve: it maintains reasonable fidelity to the underlying function, while also making reasonable progress toward the minimum (cf. Eq. (4)). These are the main points to be made using the concept of UF. It will now be quantified.

3.2 The ρ Diagnostic

Recall the GD parameter update step is

$$\theta_{new} = \theta_{old} - \alpha \nabla f,$$

where ∇f is evaluated at θ_{old} . Upon defining

$$\begin{aligned} f_{old} &= f(\theta_{old}) \\ f_{new} &= f(\theta_{new}) \\ f_{est} &= f_{old} + \nabla f \cdot d\theta, \end{aligned}$$

where $d\theta = \theta_{new} - \theta_{old}$, a generic figure for GD can be illustrated as in Fig. 2. The main insight this figure is meant to deliver is that for GD to be valid f_{est} should not be far from f_{new} , as measured on the scale of $|f_{est} - f_{old}|$. In deciding on a suitably general measure, it is also reasonable to require scale and translation invariance with respect to f . That is, multiplying f by some number shouldn't change the measure, and shifting f by some value should also not change it. (It is understood that $d\theta = \theta_{new} - \theta_{old}$ would stay fixed during such transformations of f .) Such requirements immediately disallow the obvious metrics such as an absolute error (e.g., $|f_{est} - f_{new}|$) or a relative error (e.g., $|(f_{est} - f_{new})/f_{new}|$). Instead, the following measure is introduced that consists of the error between f_{new} and f_{est} based on the scale $f_{old} - f_{est}$:

$$\rho = \left| \frac{f_{new} - f_{est}}{f_{old} - f_{est}} \right|. \quad (3)$$

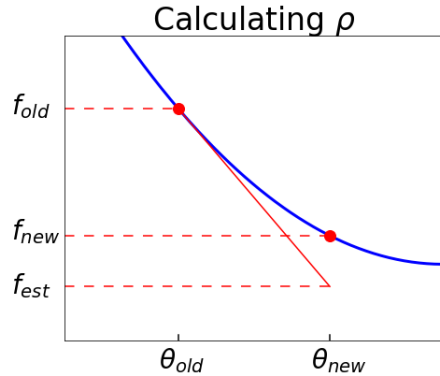


Figure 2: A depiction of the variables needed to compute ρ when θ is one-dimensional.

This definition leaves it manifestly invariant to scale and translation transformations of f , assuming $d\theta$ is fixed. By inspection, one can see that for high UF, ρ is small; when ρ is large, the UF is low. (Also, an alternative definition of ρ is given in Appendix B.)

If one does a Taylor series expansion, the leading terms comprising ρ for small $d\theta$ yield

$$\rho \rightarrow \frac{1}{2} \frac{d\theta \cdot \nabla \nabla f \cdot d\theta}{\nabla f \cdot d\theta} \sim \mathcal{O}(\alpha).$$

These results apply when f_{est} is computed using the usual first-order GD estimate. This relationship will become useful when control algorithms are developed later in the paper. The Hessian in the numerator also reveals that ρ implicitly takes into account the local curvature of f , if it wasn't already obvious from the above figure. However, ρ is not a direct measure of the curvature. Also, note that there is nothing intrinsically limiting the use of ρ to a *first-order* GD algorithm. It can be used within the context of second-order algorithms as well; in that case the above Taylor series would produce $\rho \sim \mathcal{O}(\alpha^2)$.

The diagnostic ρ may be thought of as a *quality control* parameter. When it is too small (or too large) the updates will be too small (or too large), and it will lead to a high UF (or a low UF). However, if ρ has an appropriate size, the updates will be appropriately sized, and it will lead to a moderate UF, which is the goal. For comparison, another quality control parameter from a very different context is the use of 0.05 as a cutoff for p-values in statistics. In both cases it is desirable to have it take on *small* values, but is often impractical to require that it take on values close to zero.

3.3 The *dotp* Diagnostic

As mentioned in Section 2 there is an issue with GD in that it may repeatedly overshoot the minimum, effectively zig-zagging (or oscillating) about it. A straightforward way to measure whether this is occurring is with a normalized dot product (i.e., "cosine distance") between successive updates ¹:

$$\text{dotp}_i = \frac{d\theta_{i-1} \cdot d\theta_i}{\|d\theta_{i-1}\| \|d\theta_i\|}.$$

1. It is not claimed by the author that the dotp metric is a new idea. In any event, the author has used it since 2010.

The normalization is used so it can provide a measure independent of the size of the update. Also, this diagnostic is meant to be evaluated after each iteration, since its value may rapidly change. When dotp strays from being near 1.0, it indicates the learning rate may be too large; this point will be revisited later in the paper.

The first drawback of this metric is that while dotp can easily detect a period of 2, it cannot easily reveal higher order periods ². For example, if it takes several updates for $d\theta$ to change direction, there won't be a clear indication from this metric. The second drawback is that dotp gives values independent of the scale of $\|d\theta_{i-1}\| \|d\theta_i\|$. However, this design choice is what is needed most of the time. (If it's necessary to also consider the scale, one might create the vector metric of $(\text{dotp}_i, \|d\theta_{i-1}\| \|d\theta_i\|)$). Though this metric remains valuable as-is, these drawbacks do help motivate the introduction of the *sumd* metric in the next section.

3.4 The *sumd* Diagnostic

To understand the progress of the updates of GD, it can be helpful to visualize them in θ -space. However, the dimension of θ can be extremely large, effectively precluding that possibility. Nevertheless, it will be shown in this section that a diagnostic metric can be formed from two measurables, yielding a visual depiction of the progress. With this metric, one can tell whether the updates are making progress or are exhibiting oscillations (of any periodicity). This information can help inform the decision of whether to stop the optimization run or to make some adjustments. The reader should note that this metric will not be *directly* used in forming the algorithms of this paper. However, it is related to the dotp metric, which itself may be used in conjunction with ρ . In particular, *sumd* fills in the gaps left by dotp , in that it can detect limit cycles of period greater than two, and also in that it is sensitive to the magnitude of the updates.

The *sumd* metric is a 2D curve, essentially being a *distance(d)* vs. *accumulated arclength(a)* graph, computed with respect to a reference point θ_0 . The points comprising the curve are (a_i, d_i) and are computed as

$$a_i = \sum_{k=0}^{i-1} \|d\theta_k\|$$

$$d_i = \|\theta_i - \theta_0\|,$$

where $\theta_{i+1} = \theta_i + d\theta_i$, $i = 0, 1, 2, \dots$, and a_0 is defined as 0. In words, the arclength is defined as the sum of the (magnitudes of the) differences in θ (hence the name "sumd") that lead up to θ_i starting from θ_0 . Thus, if the series of parameters is $\theta_0, \theta_1, \theta_2, \dots$, the first three points of *sumd* are

$$(a_0, d_0) = (0, 0)$$

$$(a_1, d_1) = (\|d\theta_0\|, \|\theta_1 - \theta_0\|)$$

$$(a_2, d_2) = (\|d\theta_0\| + \|d\theta_1\|, \|\theta_2 - \theta_0\|).$$

To illustrate the relationship between the path of θ and the associated *sumd* curve, consider Fig. 3, where the path is a hyperbolic spiral. Although the path of θ (left figure) was not based on GD

2. A simple remedy to detect cycles of periodicity 3 is to measure the dot product between *every other* update of θ . While this can be extended to higher order periodicities, it clearly isn't an ideal approach. In addition, a given extension would only be sensitive to that particular periodicity.

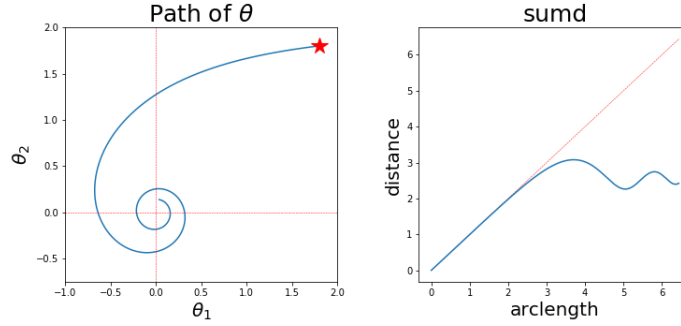


Figure 3: In the left plot, for the sake of example, the path of θ is taken to be a hyperbolic spiral. Note how the length of the path of θ continually increases as it spirals inwards, while its distance from the starting point (red star) approaches a constant. These features are reflected in the *sumd* plot on the right: the *arclength* continually increases, and the *distance* oscillates while approaching a constant value.

updates, it should be imagined that way for the purpose of this example. The path of θ begins at the red star and spirals down toward the origin. Initially, the arclength and the distance are nearly equal; this is because there is little initial curvature in the path of θ . However, as the path begins to spiral, the distance from the initial point reaches a maximum, while the arclength continues to grow. Following that, the distance decreases, then increases again, etc. This oscillation on the right hand side of Fig. 3 is generically indicative of a limit cycle in θ -space. Clearly, the construct of this metric is easily capable of detecting a cycle of any periodicity.

At any given step the arclength (a_i) is greater than or equal to the distance (d_i) from the reference point θ_0 . This is easily seen from

$$a_i = \sum_{k=0}^{i-1} \|d\theta_k\| \geq \left\| \sum_{k=0}^{i-1} d\theta_k \right\| = \|\theta_i - \theta_0\| = d_i .$$

It is also easily understood from intuition that these individual steps $d\theta$ produce a maximal length vector when they all point in the same direction. In any case, this is why the *sumd* curve lies below the 45 degree line; a red dotted line at 45 degrees in the *sumd* plot is added as a visual reference. To summarize, if the path of θ is experiencing a curve relative to $(\theta - \theta_0)$, it will be reflected by the *sumd* curve veering away from 45 degrees. If this path later straightens out, the *sumd* curve will again advance at a 45 degree angle (although now it will be displaced beneath the 45 degree red-dotted line in the figure).

It should be remembered that the horizontal axis is *not* the number of iterations. The points of *sumd* are *not* required to march along at a constant rate from left to right; in fact, they typically don't do so. Instead, it is often the case that initial updates of θ are large, and are later followed by relatively small changes. Indeed, at some point it may even show that the changes have effectively become zero. To help identify these varying changes in later *sumd* figures, thin vertical lines will be added after a set number of updates; this will help display the rate of progress.

4. Computing ρ

A quick inspection of the formula for ρ shows that it depends on two successive values of the CF. It might then seem that in order to incorporate it into a typical optimization loop, another evaluation of the CF would be necessary. However, this is not the case. First, recall the standard sequence of steps for the optimization of a CF using GD as shown in Algo. 1.

Algorithm 1 : Sequence of operations for a basic GD algorithm

```

Init:  $\theta$ 
for  $i = 1$  to  $num+1$  do
   $f = f(\theta)$ 
   $g = \nabla f(\theta)$ 
   $d\theta = -\alpha g$ 
   $\theta = \theta + d\theta$ 
end for
Return:  $\theta$ 

```

Here, some of the steps that are normally combined are on separate lines, in order to more easily compare with later pseudocode. Also, dependence on other variables for these function calls is suppressed (e.g., the data, cached variables, etc.), as well as steps such as reading in the data and initializing the parameters (θ , α , etc.). The "stopping condition" may depend on f , g , etc. It's left out for simplicity; instead a fixed number of iterations is used. Finally, the number of iterations is set to $num+1$, to make the comparison easier for the following pseudocode.

In Algo. 1, the most important feature to notice is the ordering of these computations within the loop: f ; g ; $d\theta$; update of θ . The approach now will be to do an initial computation of the CF before entering the loop, but to otherwise respect the order. Thus, inside the new loop, the order of the computations is: g ; $d\theta$; update of θ ; f . This rewriting allows one to easily access the old and new values of f , and so compute ρ with essentially *no* new steps. Again, this approach is convenient because ρ (and for that matter dotp and sumd), are computed "between steps". With these changes, the standard algorithm to be used now is shown in Algo. 2:

Algorithm 2 : Amended basic GD algorithm, now including computation of ρ

```

Init:  $\theta_{old}$ 
 $f_{old} = f(\theta_{old})$ 
for  $i = 1$  to  $num$  do
   $g = \nabla f(\theta_{old})$ 
   $d\theta = -\alpha g$ 
   $\theta_{new} = \theta_{old} + d\theta$ 
   $f_{new} = f(\theta_{new})$ 
   $f_{est} = f_{old} + g \cdot d\theta$ 
   $\rho = \text{get\_rho}(f_{old}, f_{new}, f_{est})$ 
   $f_{old} = f_{new}$ 
   $\theta_{old} = \theta_{new}$ 
end for
Return:  $\theta_{new}$ 

```

The function `get_rho` refers to Eq. (3). This is perhaps the simplest rewriting of Algorithm 1 in order to compute ρ without extra computation; alternatives might include performing additional steps before entering the main loop, such as the computation of the gradient³. One might find a variation to be more convenient if also computing the other diagnostics (`dotp` and `sumd`), which were left out here for simplicity. Finally, as an exercise, one can verify that for a small value of `num` that each algorithm computes the CF the same number of times.. Actually, the new ordering may be preferable, since the final value of θ corresponds to the final value of the CF; in the former case it doesn't.

5. Solutions for Simple Cases

The purpose of this section is to build an understanding of the use of these metrics by applying them to several simple examples. Particular attention will be paid to the relationship between α and ρ . In the discussion that follows, the value of ρ will be compared to a *target interval*, which is defined as

$$(\rho_{min}, \rho_{max}) = (0.015, 0.15). \quad (4)$$

This is meant to correspond to a "moderate UF", as defined earlier. This range for ρ is meant as a guide, based on the experience of the author; the values weren't derived from other considerations. In comparison to remarks made in Sec. 3.1, this range of ρ is meant to ensure *reasonable* progress with a *reasonable* fidelity.

In the algorithms of this paper, attempts will be made to keep ρ equal to a target value (ρ_{targ}). As a matter of definition, when it's possible to maintain $\rho = \rho_{targ}$ throughout the optimization run, the setting of α will be called *ideal*. Thus, the notion of *ideal* is with respect to the ansatz. When it's only possible to maintain $\rho \in (\rho_{min}, \rho_{max})$ (even approximately), the setting of α will be called *near-ideal*. In this paper the value of $\rho_{targ} = 0.1$ will be used.

5.1 Quadratic

In this section, the CF is a quadratic function of an n-dimensional parameter $\theta = (\theta_1, \dots, \theta_n)$. The CF is defined as $f = c\theta \cdot \theta = c\theta^2$, where c is a positive constant. An update from θ to $\theta + d\theta$ using GD leads to

$$\begin{aligned} d\theta &= -\alpha \nabla f = -2\alpha c\theta \\ f_{old} &= c\theta^2 \\ f_{new} &= c(\theta + d\theta)^2 \\ f_{est} &= f_{old} + \nabla f \cdot d\theta. \end{aligned}$$

Using these expressions in Eq. (3) and recalling $\alpha > 0$ leads to

$$\rho = \alpha c. \quad (5)$$

It may be puzzling to the reader why the constant c appears in this, when by construction ρ should have no dependence on the scale of f . However, in that earlier argument it was required that $\|d\theta\|$ be held constant, which is not the case here. Also, in later examples it will be seen that ρ may carry a dependence on θ .

3. For example, after the update of θ in Algo. 1, one could add an "IF $i > 1$ " conditional which computes f_{est} and ρ . Following that, set $f_{old} = f$.

The combination αc in Eq. (5) is interesting since it implies that ρ can have the same value for cases where α is very different. Eg, $\alpha = 0.1$ and $c = 5$ will produce the same value for ρ as $\alpha = 10$ and $c = 0.05$. This may help partially explain why a choice of α that gives good results in one application may give poor results in another⁴. In any event, it already appears from just one example that ρ , not α , is a better "universal parameter" by which to make comparisons between applications.

Even though this is an elementary example, one should not miss the conceptually important point that is now possible to formulaically determine a value for the learning rate, vis-à-vis $\alpha = \rho/c$, in which it depends only on a "quality control" parameter ρ and a constant. This is fundamentally different from the usual approach, in which one tries a number of different values for α , and makes a subjective decision based on the shape of a *training error vs. iterations* plot. In contrast, by using ρ it is possible to set α in an *a priori* fashion.

As this is a basic example, it's possible to further quantitatively evaluate the dependence on ρ using an exact solution. (In particular, the substitution $\alpha = \rho/c$ will be assumed.) The value of θ at the t th iteration (beginning from $t = 0$) equals

$$\begin{aligned}\theta_t &= \theta_{t-1} + d\theta_{t-1} \\ &= (1 - 2\rho)\theta_{t-1} \\ &= (1 - 2\rho)^t\theta_0.\end{aligned}$$

This reveals how the updates, upon increasing ρ , become oscillatory when $\rho > 1/2$ and become divergent when $\rho > 1$. The period-2 oscillatory nature of θ_t when $\rho > 1/2$ is also evident from the dotp diagnostic:

$$\text{dotp}_t = \text{sign}(1 - 2\rho).$$

In addition, the log of the CF at the t th iteration equals

$$\log f_t = 2t \log |1 - 2\rho| + \log c\theta_0^2.$$

So in a plot of $\log f_t$ vs. t , the slope should be $2 \log |1 - 2\rho|$ and the intercept $\log c\theta_0^2$. Thus, the closer ρ is to 0.5, the faster the CF decreases.

Next, the sumd plot is examined in Fig. 4 using $\rho = 0.1$ and $\rho = 0.8$. As expected, the plot for $\rho = 0.1$ shows a steady progression along the 45 degree line, since the updates take a direct path toward the minimum at $\theta = 0$. In the right-hand plot with $\rho = 0.8$, the graph reveals the characteristics of an oscillation in parameter space: the arclength continually increases while the distance oscillates. Note it is not necessary to know the period of the oscillations beforehand in order to detect them with sumd. In both cases the vertical red lines were added (after every 10 iterations) so the reader could more easily assess the progress. Also, the values of (a, d) in the plots appear as the blue points. Finally, plots of dotp were not shown since they were especially simple: for $\rho < 0.5$, dotp=1, and for $\rho > 0.5$, dotp=-1.

5.2 Quartic

Here the CF is defined as $f = c\theta^4 \equiv c(\theta \cdot \theta)^2$, and a GD update is $d\theta = -4\alpha c\theta^2\theta$. Following the same approach from the last section, ρ is computed as

$$\rho = 6q - 16q^2 + 16q^3, \tag{6}$$

4. This could partially be mitigated by a suitable normalization of the CF beforehand.

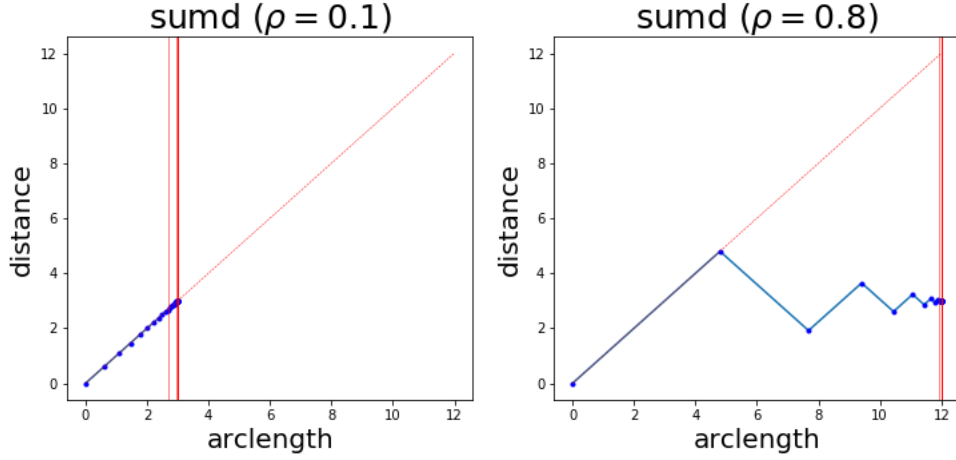


Figure 4: In the left plot with $\rho = 0.1$, the updates directly approach the minimum. On the right plot, where $\rho = 0.8$, the updates oscillate as they approach the minimum.

where $q = \alpha c \theta^2$. The fact that ρ depends on the combination $\alpha c \theta^2$ reveals a dependency that may not have been appreciated hitherto. Inverting this equation while assuming small q and ρ reveals, approximately:

$$\alpha = \rho / (6c\theta^2). \quad (7)$$

Thus, once again, α may be expressed in an a priori way as a function of ρ . What is new is that α now also depends on θ . This means that, in order to maintain a certain value of ρ , α must be continually adjusted while taking θ into account. It also means that a suitable α for one initial θ may be wholly inappropriate for a different initial θ . Once again, it becomes apparent that ρ , not α , is a better universal measure for characterizing an optimization run.

Upon using α from Eq. 7, the t th update for θ becomes

$$\begin{aligned} \theta_t &= \theta_{t-1} + d\theta_{t-1} \\ &= \theta_{t-1} - 4\alpha c \theta_{t-1}^2 \theta_{t-1} \\ &= (1 - 4q)^t \theta_0. \end{aligned}$$

This formula predicts converging oscillations when $q > 1/4$, which become diverging when $q > 1/2$; using Eq. (6) these values are equivalent to $\rho = 0.75$ and $\rho = 1.0$, respectively. This formula leads to this expression for the log of the CF at the t th update

$$\log f_t = 4t \log |1 - 4q| + \log c\theta_0^4.$$

Keep in mind that this is true when α is adjusted according to $\alpha = q/(c\theta^2)$. The algorithm that results when α is adjusted this way is named "Ideal GD"; it is compared against GD (here called "Basic GD") in Fig. 5. The Basic GD algorithm used $\alpha = 0.01$, and the Ideal GD used $q = 0.02$ (or equivalently $\rho \approx 0.114$, according to Eq. (6)). The plots reveal that Ideal GD leads to a far smaller value of $\log f$, by about 10 orders of magnitude. In the $\log \rho$ plot, it was revealed that Basic GD did not keep ρ in the target interval of (ρ_{min}, ρ_{max}) ; in fact, it has no apparent control over this

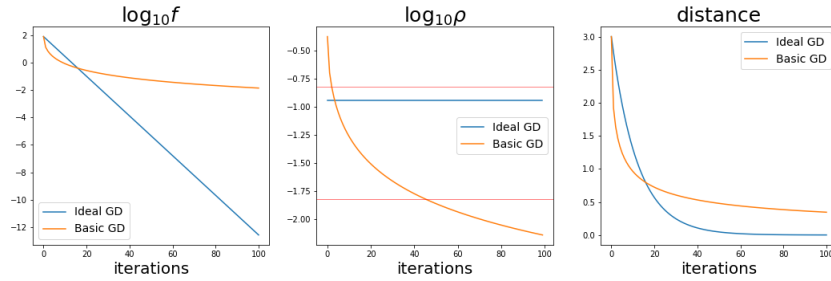


Figure 5: A comparison on the quartic CF with $c = 1$ between Basic GD using $\alpha = 0.01$ vs. an Ideal GD using $q = 0.02$ (or equivalently $\rho \approx 0.114$).

metric. (The decrease of ρ for Basic GD and the appearance of a plateau for $\log f$ will be seen to be a recurring criticism of the GD family of algorithms in this paper.) In contrast, the Ideal GD had a constant value of $\log \rho$ (equal to $\log(0.114\dots)$), by construction. The third plot of the figure tracks the distance between the initial $\theta = -3$ and the minimum ($\theta = 0$); Ideal GD again outperforms Basic GD. Finally, note that Eq. (7) also leads to α becoming increasingly large for Ideal GD, as it now grows as $\alpha \sim \theta_t^{-2}$.

5.3 Ellipse

Working in two dimensions with $\theta = (\theta_1, \theta_2)$, the CF for the ellipse is

$$f(\theta) = (\theta_1/a)^2 + (\theta_2/b)^2,$$

where $a, b > 0$. The update step from basic GD is $d\theta = -\alpha \nabla f = -2\alpha (\theta_1/a^2, \theta_2/b^2)$. Computing ρ using Eq. (3) leads to $\rho = (\alpha Q_6)/Q_4$ where

$$Q_m = \frac{\theta_1^2}{a^m} + \frac{\theta_2^2}{b^m}.$$

This result immediately leads to a formula for adjusting α according to the changing value of θ , and a pre-set value of ρ :

$$\alpha = \frac{Q_4}{Q_6} \rho. \quad (8)$$

This dynamically-set α is used in an "Ideal GD" algorithm, and is compared to Basic GD in Fig. 6 when applied to the ellipse CF. Once again, Ideal GD leads to a lower value for $\log f$ by many orders of magnitude. Also, as with the quartic CF, the derived ρ for Basic GD is seen to drop below the target range, taking on very small values. This small ρ explains why the approach toward the minimum by Basic GD in the distance plot is much slower than for Ideal GD. In this case the distance is measured with respect to the minimum at $(0, 0)$.

5.4 Summary

These simple examples have demonstrated that it's possible to solve for α as a function of ρ . This is a unique situation: it means the learning rate can be set at each iteration, and will depend not just on

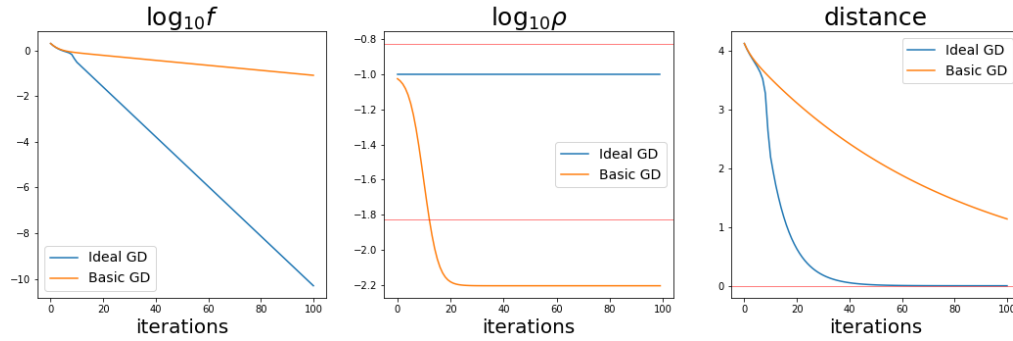


Figure 6: Comparison plots between Basic GD (using $\alpha = 0.1$) and Ideal GD using α set according to Eq. (8) with $\rho = 0.1$. In both cases the initial θ was $(4, 1)$, and $a = 4$, $b = 1$.

θ , but also the diagnostic metric ρ . Of course, for more complex CFs, it won't be possible to obtain an exact solution for $\alpha(\rho)$ as has been done here. Nevertheless it will be shown how to obtain similar results.

These results establish the approach of the *constant ρ ansatz* that will be used going forward: at each iteration adjustments will be made to keep ρ at a fixed target value (as much as possible). Indeed it was seen to be very successful in these simple cases, with the value of the $\log f$ decreasing at a linear rate, far outstripping the results of Basic GD for the quartic and ellipse CFs. (The results were identical for the trivial quadratic CF since there $\alpha \sim \rho$.) Such a linear descent in $\log f$ is taken as a *gold standard* for algorithms based on GD.

6. Algorithms

6.1 Setting the Learning Rate Dynamically

The approach in this section is to seek a means to isolate a formula for α in a manner similar to what was done in the previous section. Of course, for realistic examples, the CF will have a complicated dependence on α , and so a slightly varied strategy may be required. Also, a side goal in this approach is to avoid any additional computation, as much as possible. It is noted that

$$\begin{aligned} f_{new} - f_{est} &= \mathcal{O}(\alpha^2) \\ f_{est} - f_{old} &= \mathcal{O}(\alpha). \end{aligned}$$

This follows from the Taylor series expansion of f . Next, the leading α -dependence is pulled out by defining the following quantities

$$\begin{aligned} A &= (f_{new} - f_{est})/\alpha^2 \\ B &= (f_{est} - f_{old})/\alpha. \end{aligned}$$

Observe that A and B involve little additional computation. Recall that from the re-writing of GD in Algo. 2, f_{old} and f_{new} are already available, and f_{est} is easily found. To lowest order in α , A is a constant. However it does in general retain α -dependence. Also, B is a constant; it equals $-\|\nabla f\|^2$

and has no α -dependence. With these definitions, the original equation for ρ (i.e., Eq. 3) becomes

$$\rho = \left| \frac{\alpha A}{B} \right|.$$

This immediately yields a solution for α , which is used to define a function h

$$\alpha = h(A, B, \rho) \equiv \left| \frac{B}{A} \right| \rho. \quad (9)$$

This will be called the *adaptation formula* for α .

Finally, though it's a moot point since A is inside absolute value signs, the sign of A depends on the concavity of f . When f is *concave down*, $f_{est} > f_{new}$; when it's *concave up*, $f_{est} < f_{new}$. In both cases, by construction, one expects that $f_{new} < f_{old}$ and $f_{est} < f_{old}$. It follows that if f is concave up (down), the sign of A is $+1(-1)$. In contrast, the sign of B is always -1 . Also, in all cases, ρ and α are positive by construction.

6.2 Using the Adaptation Formula

The adaptation formula just introduced requires the computation of f_{new} , f_{old} and f_{est} , and can be computed *after* an update of θ has already been done. This isn't quite as convenient as with the Ideal GD algorithms used with the simple functions discussed earlier. Nevertheless, it is still useful in that it can be used in the *subsequent* iteration as an *approximate* α . This approximation will work well provided $A(\alpha)$ doesn't change too rapidly.

A slightly more detailed way of understanding the situation is the following. Suppose an iteration has completed, and α , A , B and ρ are known. It follows that these quantities exactly satisfy the adaptation formula

$$\alpha = h(A, B, \rho).$$

In general, this ρ will be different from its target value, ρ_{targ} . What is sought here is the ability to change ρ to a new value, and from the equation compute the new α to be used. Calling these new values α' , ρ' , and $A' = A(\alpha')$, the new adaptation equation would appear as

$$\alpha' = h(A', B, \rho').$$

(Recall B is independent of α .) As an approximation to this, on the assumption that A isn't changing too rapidly with respect to α , one can write

$$\alpha'_0 = h(A, B, \rho'). \quad (10)$$

It is expected that so long as ρ and ρ' are sufficiently close, α'_0 will be a good approximation to α' (Zimmer, 2020a).

The planned use of this equation in an optimization algorithm is summarized as follows. After an iteration, the quantities A , B , and ρ are computed. If ρ isn't too different from ρ_{targ} , the value $\rho' = \rho_{targ}$ is used in Eq. (10) to compute α'_0 , which will be the learning rate used in the following iteration. This is the essence of the Neograd_v0 algorithm to be introduced in the next section. However, if ρ differs too significantly from ρ_{targ} , a different value for ρ' will be used instead, one that is somewhere between the values of ρ and ρ_{targ} . That heuristic is done to recognize that Eq. (10) has a limited range of usefulness as an approximation. This is the approach taken in Neograd_v1, also to be introduced below.

6.3 Neograd_v0

As alluded to in the previous section, this algorithm will compute the learning rate to be used in the *subsequent* iteration using $\alpha = h(A, B, \rho_{targ})$, where h was defined in Eq. (9). As a convenience in this program, h is implemented with `get_h` in Algo. 3, and accepts slightly different inputs

Algorithm 3 : `get_h`

Input: $(f_{old}, f_{new}, f_{est}, \alpha, \rho')$
 $A = (f_{new} - f_{est})/\alpha^2$
 $B = (f_{est} - f_{old})/\alpha$
 $\alpha' = \rho'|B/A|$
Return: α'

The `Neograd_v0` algorithm is defined in Algo. 4.

Algorithm 4 : `Neograd_v0`

Input: $(\theta_{old}, \alpha, \rho_{targ}, \text{num})$
 $f_{old} = f(\theta_{old})$
for $i = 1$ to num **do**
 $\mathbf{g} = \nabla f(\theta_{old})$
 $d\theta = -\alpha \mathbf{g}$
 $\theta_{new} = \theta_{old} + d\theta$
 $f_{new} = f(\theta_{new})$
 $f_{est} = f_{old} + \mathbf{g} \cdot d\theta$
 $\alpha = \text{get_h}(f_{old}, f_{new}, f_{est}, \alpha, \rho_{targ})$
 $f_{old} = f_{new}$
 $\theta_{old} = \theta_{new}$
end for
Return: θ_{new}

As already mentioned, this algorithm is expected to work well (and will be shown to do so) in cases where A doesn't change too rapidly with respect to α . This algorithm represents the simplest way to use Eq. (9).

6.4 Neograd_v1

This algorithm is a refinement on `Neograd_v0`, in that when the initial ρ differs too greatly from ρ_{targ} , it doesn't try to make the adjustment in a single step. Instead, it uses a heuristic to make a partial adjustment. It has been the experience of the author that this is more critical when $\rho \ll \rho_{targ}$. Also, when $\rho < \rho_{targ}$, the main risk is that the algorithm will simply become inefficient, as the updates aren't as large as they could be. On the other hand, when $\rho > \rho_{targ}$, there is a risk that the updates will cause θ to leave its local basin of attraction, which in general should be avoided (see Sec. 2.2). Thus, as a simplification for exposition, when $\rho > \rho_{targ}$, the next value of ρ will be immediately set to ρ_{targ} . This logic of choosing a new value for ρ is captured in Algo. 5

Algorithm 5 : get_rho_prime

```

Input:  $(\rho, \rho_{targ})$ 
if  $\rho < \rho_{targ}$  then
   $r = 0.75 \log_{10}(\rho / \rho_{targ})$ 
   $\rho' = 10^r \rho_{targ}$ 
else
   $\rho' = \rho_{targ}$ 
end if
Return:  $\rho'$ 

```

For example, when $\rho = 10^{-9}$ and $\rho_{targ} = 0.1$, it returns $\rho' = 10^{-7}$. So with respect to log values, ρ' is 3/4 of the way to ρ and 1/4 to ρ_{targ} . The Neograd_v1 algorithm can now be defined in Algo. 6:

Algorithm 6 : Neograd_v1

```

Input:  $(\theta_{old}, \alpha, \rho_{targ}, \text{num})$ 
 $f_{old} = f(\theta_{old})$ 
for  $i = 1$  to  $\text{num}$  do
   $\mathbf{g} = \nabla f(\theta_{old})$ 
   $d\theta = -\alpha \mathbf{g}$ 
   $\theta_{new} = \theta_{old} + d\theta$ 
   $f_{new} = f(\theta_{new})$ 
   $f_{est} = f_{old} + \mathbf{g} \cdot d\theta$ 
   $\rho = \text{get\_rho}(f_{old}, f_{new}, f_{est})$ 
   $\rho' = \text{get\_rho\_prime}(\rho, \rho_{targ})$ 
   $\alpha = \text{get\_alpha\_prime\_0}(f_{old}, f_{new}, f_{est}, \alpha, \rho')$ 
   $f_{old} = f_{new}$ 
   $\theta_{old} = \theta_{new}$ 
end for
Return:  $\theta_{new}$ 

```

In this algorithm, the computation of the diagnostics (dotp, sumd, etc.) was suppressed for simplicity. There are (at least) two ways that get_rho_prime can be improved, so as to better deal with CFs that exhibit extremely challenging features (i.e., either extremely flat or steep). The first is to recognize that the number 0.75 in Algo. 5 is adjustable. When it is closer to 1.0 it is better able to handle rapidly changing CF landscapes. The second is to recognize that for both cases ($\rho < \rho_{targ}$ and $\rho > \rho_{targ}$) it is prudent to verify that the proposed α actually leads to an acceptable ρ ; this may require a repeat calculation (cf. Neograd_dbl).

6.5 Neograd_dbl

"Double, double toil and trouble..." (Shakespeare)

Neograd_dbl is a refinement that can be based on either Neograd_v0 or Neograd_v1; in this section it is based on v1. The idea of this refinement is to repeat some of the steps in the main loop, so that a more accurate estimate of α can be found. This means that when Eq. (10) is used, the current and

target ρ will in general not be as different. As Algo. 7 shows, a portion of the loop is repeated $nrep$ times. It is suggested to only use $nrep=2$, since there will be diminishing returns when setting it higher. (Computations in this loop will be expensive for a real application.)

Algorithm 7 : Neograd_dbl

```

Input: ( $\theta_{old}, \alpha, \rho_{targ}, nrep, num$ )
 $f_{old} = f(\theta_{old})$ 
for  $i = 1$  to  $num$  do
   $\mathbf{g} = \nabla f(\theta_{old})$ 
  for  $j = 1$  to  $nrep$  do
     $d\theta = -\alpha \mathbf{g}$ 
     $\theta_{new} = \theta_{old} + d\theta$ 
     $f_{new} = f(\theta_{new})$ 
     $f_{est} = f_{old} + \mathbf{g} \cdot d\theta$ 
     $\rho = \text{get\_rho}(f_{old}, f_{new}, f_{est})$ 
     $\rho' = \text{get\_rho\_prime}(\rho, \rho_{targ})$ 
     $\alpha = \text{get\_alpha\_prime\_0}(f_{old}, f_{new}, f_{est}, \alpha, \rho')$ 
  end for
   $f_{old} = f_{new}$ 
   $\theta_{old} = \theta_{new}$ 
end for
Return:  $\theta_{new}$ 

```

Note that when $nrep=1$, this becomes Neograd_v1. This algorithm involves a trade-off between the increased time of computation of the inner loop portion versus the benefits of a more accurate assessment of an appropriate α . For CFs with a challenging landscape, it may be advantageous to have this extra control. Finally, it has to be noted that this method isn't fool-proof; it's still possible for it to produce a ρ that exceeds ρ_{targ} . This will be seen in the initial iterations of Figs. 19 and 20.

6.6 Hybrid Versions

The most essential aspects of the above Neograd algorithms can be combined with existing algorithms of the GD family. For example, Neograd_v1 can be combined with GD family algorithms, as shown in Algo. 8

Algorithm 8 : Neo*

```

Input:  $(\theta_{old}, \alpha, \rho_{targ}, num, type\_opt)$ 
 $f_{old} = f(\theta_{old})$ 
 $v = \mathbf{0}, v2 = \mathbf{0}$ 
for  $i = 1$  to  $num$  do
   $g = \nabla f(\theta_{old})$ 
   $d\theta, v, v2 = \text{get\_dp\_combo}(type\_opt, g, \theta_{old}, v, v2, i, \alpha)$ 
   $\theta_{new} = \theta_{old} + d\theta$ 
   $f_{new} = f(\theta_{new})$ 
   $f_{est} = f_{old} + g \cdot d\theta$ 
   $\rho = \text{get\_rho}(f_{old}, f_{new}, f_{est})$ 
   $\rho' = \text{get\_rho\_prime}(\rho, \rho_{targ})$ 
   $\alpha = \text{get\_alpha\_prime\_0}(f_{old}, f_{new}, f_{est}, \alpha, \rho')$ 
   $f_{old} = f_{new}$ 
   $\theta_{old} = \theta_{new}$ 
end for
Return:  $\theta_{new}$ 

```

The function `get_dp_combo` is a compact writing of the GD family algorithms (see Table 1). In the argument list for this function, v and $v2$ represent the exponential weighted averages of the first and second moments of g , respectively. For example, for NeogradM, v is used, but $v2$ is not; for Adam both are used. The variable `type_opt` is used to indicate which GD family algorithm is being combined with a Neograd algorithm. (The usual parameters β, β_2, ϵ used for Adam are suppressed in this pseudocode.) The actual implementation is available elsewhere (Zimmer, 2020b). Also, as alluded to, while the above Algo. 8 is based on `Neograd_v1`, it could be based on `Neograd_v0`. A suggested naming rubric for the hybrid algorithms is in Table 1. To clarify which version of Neograd

Original name	New name
Basic GD	Neograd
GD + momentum	NeogradM
GD + Nesterov momentum	NeoNAG
RMSProp	NeoRMS
Adam	NeoAdam

Table 1: Corresponding names for the original and new versions of the algorithm, as based on Neograd

is being hybridized, one might consider appending the suffix `_v0`, `_v1`, or `_dbl`, according to which member of the "Neograd family" is being used.

6.7 Choosing an Initial α

No matter which optimization algorithm is used (from the Neograd or GD family), it is convenient to begin with an α that immediately leads to an acceptable value of ρ . Note that in the absence of the algorithms that have been introduced in this paper, one wouldn't have a way to assess whether a given value for α was appropriate before launching into an optimization run. As explained earlier,

the modus operandi in that case was to just do several runs and choose the α corresponding to the "best" run.

However, given that the metric ρ is available, which can assess the appropriateness of an α using only two measurements of the CF, an entirely more effective approach becomes possible. One can now simply choose an initial θ and α , and measure the CF before and after an update. If the resulting ρ between those two measurements is too large or small, it can just be adjusted appropriately. There are a variety of ways of accomplishing such an approach, and they can be adjusted in order to provide different levels of *simplicity* or *robustness*. Perhaps the simplest is just to borrow elements of Neograd_dbl: in particular the inner loop that adjusts α nrep times. This approach is shown in Algo. 9

Algorithm 9 : get_starting_alpha

```

Input: ( $\theta_{old}$ ,  $\alpha$ ,  $\rho_{targ}$ , nrep)
 $f_{old} = f(\theta_{old})$ 
 $\mathbf{g} = \nabla f(\theta_{old})$ 
for j = 1 to nrep do
     $d\theta = -\alpha\mathbf{g}$ 
     $\theta_{new} = \theta_{old} + d\theta$ 
     $f_{new} = f(\theta_{new})$ 
     $f_{est} = f_{old} + \mathbf{g} \cdot d\theta$ 
     $\rho = \text{get\_rho}(f_{old}, f_{new}, f_{est})$ 
     $rerr = (\rho - \rho_{targ}) / \rho_{targ}$ 
     $\rho' = \text{get\_rho\_prime}(\rho, \rho_{targ})$ 
     $\hat{\alpha} = \alpha$ 
     $\alpha = \text{get\_alpha\_prime\_0}(f_{old}, f_{new}, f_{est}, \alpha, \rho')$ 
end for
Return: ( $\hat{\alpha}$ , rerr)

```

This function should be called before entering the main loop in any of these optimization algorithms. Since Algo. 9 should be called at the start of a run, there's no need for exponential weighted averages, and get_dp_combo in Algo. 8 was replaced with Basic GD. Note there are a number of ways to write this kind of algorithm. For example, the for-loop can be replaced with a while-loop, with a break condition based on rerr, or on whether ρ is in an acceptable range (cf. Eq. (4)). Also, note that this algorithm takes a starting α as one of its inputs. The author has found it's beneficial to choose this starting value to be overly small. With a value that's too large, it's possible to have an update that skips over a minimum in the CF profile, and yet still produces a ρ that's within the target interval; such a situation is to be avoided. In particular, the initial α should preferably produce a ρ that is less than ρ_{min} .

An increasing amount of sophistication can be layered on top of get_rho_prime in Algo. 9. For example, as already mentioned, in the code branch where $\rho < \rho_{targ}$, the constant 0.75 could be made adjustable, perhaps to reflect other variables. Also, in the section where $\rho > \rho_{targ}$, ρ could be set to something smaller than ρ_{targ} (perhaps as a function of ρ_{targ}/ρ). In addition, in either case, a second computation of the CF could be done to refine the estimate, in a manner similar to what was done with Neograd_dbl. Doing this would provide an increased level of robustness that might be

warranted for the most challenging CF landscapes (cf. Sec. 7.5). An implementation with additional features is available elsewhere (Zimmer, 2020b).

7. Experiments

In this section various test functions and a NN model are used to evaluate and compare the various algorithms that have been introduced. While the test functions are fairly simple, they provide a clean window into the operating of the algorithm, thereby revealing their strengths and weaknesses. However, it is also suggested that in the course of an optimization run, a CF for an actual application will at times approximate one or more of these test functions. Thus, they potentially serve as a partial proxy for an actual CF.

There are a large number of potential comparisons that can be made between all the different algorithms on all the different CFs. However, it is not the purpose of this paper to make such an exhaustive study. Instead, this section will examine certain algorithms or scenarios associated with the CFs of interest. This is done to illustrate a point, or to highlight a comparison. However, it will be the case that most comparisons will be between Adam and NeogradM, as Adam is a current popular choice, and NeogradM seems to be the best performing of the Neograd family (excluding those with repeat computations, such as NeogradM_dbl).

An effort was made to find the "best" learning rate for algorithms of the GD family to make a fair comparison to those of the Neograd family. Remaining parameters for Adam were set to their default values (i.e., $\beta = 0.9$, $\beta_2 = 0.999$, $\epsilon = 10^{-8}$). (Finding a best α wasn't necessary with the Neograd family.) The best values are defined as those leading to the lowest value CF while generally exhibiting stable behavior throughout. Also, the diagnostics `dotp` and `sumd` were used to help evaluate stability. In addition, all algorithms were evaluated with respect to the ρ diagnostic. Recall that the sought-after behavior of ρ is that it remain in the target interval (ρ_{min}, ρ_{max}) , as defined in Eq. (4). Also, recall that excursions of ρ below ρ_{min} are judged as merely inefficient, while those above ρ_{max} are deemed potentially hazardous. Finally, in some cases a plot will be made of the $\log(\text{distance})$, where $\text{distance} = \|\theta_t - \theta_{min}\|$, θ_t is the current parameter value, and θ_{min} corresponds to the minimum of the CF (assuming it's known).

7.1 Quartic

The quartic CF is perhaps the simplest CF in which interesting differences begin to appear; the quadratic is a bit too simple. In Fig. 7 are shown the most compelling contrasts between Adam and NeogradM. The log of the CF on the left shows that NeogradM leads to linear descent (cf. Ideal GD in Fig. 5); the profile due to Adam is that of fast initial descent, followed by a near plateau. This switch-over occurs near the `iterations=50` mark, and leads to significant consequences: after 200 iterations there is an approximately 15 order of magnitude ratio between the two CF values. This behavior is mirrored in the $\log(\text{distance})$ plot, which shows that NeogradM is capable of bringing θ very close to $\theta = 0$, whereas Adam is not.

The reason for this plateau can be understood from the middle plot, that of $\log \rho$. Recall that the ideal value for $\log \rho$ should be between the red lines, which define the interval $(\log \rho_{min}, \log \rho_{max})$. For Adam, ρ is seen to drop precipitously near `iterations=50`. Recall that this means it is exhibiting high UF, and the updates are overly conservative. (By contrast, observe that NeogradM maintains a nearly constant value within the interval.)

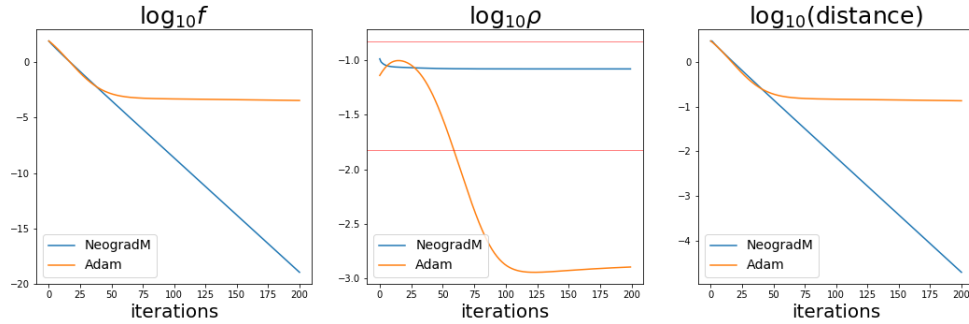


Figure 7: Plots of NeogradM vs. Adam for a quartic CF. The parameter begins at $\theta = -3$; the minimum is at $\theta = 0$.

These plateaus in the CF and distance plots will be seen to be a recurring theme in the GD family algorithms. They essentially implement an *early stopping* form of regularization, and greatly limit the performance of the optimization. At present it is unclear why they behave in this way.

7.2 Sigmoid-well

In the other experiments of this paper comparisons are made between different algorithms. This section is unique, in that it will focus on one algorithm (NeogradM) and attempt to shed light on its behavior by examining how α changes in response to a challenging CF.

The CF itself is composed of two sigmoid functions: one increases to the left, and one to the right; they are shifted and added. Together they produce the CF f , which is named *sigmoid-well*:

$$f(\theta) = \sigma[s(-\theta - a)] + \sigma[s(\theta - a)]$$

$$\sigma(\bullet) = 1/(1 + e^{-\bullet}).$$

(Note that θ is a 1-dim vector and is written as θ .) The motivation for this CF was to test an algorithm in scenarios that are notoriously difficult for GD family algorithms, that of very flat and steep CF landscapes. The parameters s and a control the steepness and location of the drop, respectively; they're set to $s = 10$ and $a = 2$. Fig. 8 reveals these features: In the optimization run to be discussed, the initial parameter value is $\theta = -3$, and is marked by a red star in this figure. The minimum occurs at $\theta = 0$ and is marked by a black star. The updates in the optimization to be discussed will take θ from the red star, past the inflection point near $\theta = -2$, and eventually close to the black star. The plots of the CF, θ and α together tell a story of the optimization run, as shown in Fig. 9. In the plots, vertical red lines are drawn in at *iterations* = 55 and 171. As shown in the rightmost figure, they correspond to turning points in the behavior of $\log \alpha$ vs *iterations*. The turning points can be understood by examining the plots of f and θ vs. *iterations*. Note that near *iterations*=50 in the leftmost plot, the CF has dropped to near 0; at that point θ is still between -1.5 and -2.0. Also, θ won't be close to the minimum at 0 till about *iterations* = 170. Given these observations, the sharp descents and ascents of $\log \alpha$ in the rightmost plot are now understandable. Near the beginning of the optimization run, the updates of θ are just beginning to lead to a drop in the CF. (The initial increase of α in the rightmost plot of Fig. 9 is due to the fact that the starting α was chosen to be relatively small.) Because this is such a steep descent, α must be reduced quickly; that is exactly what is seen

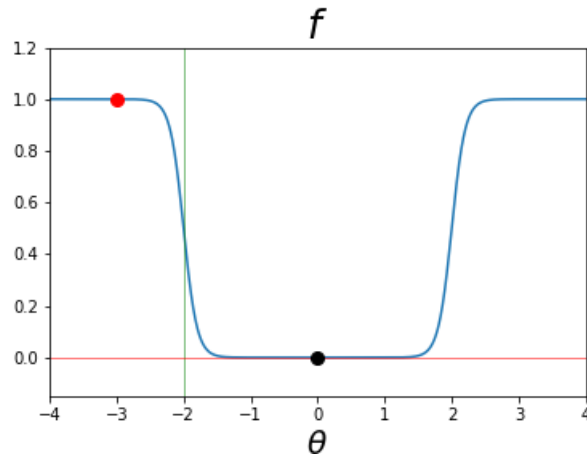


Figure 8: Profile of the CF *sigmoid-well*. Updates begin at $\theta = -3$ (red star) and approach the minimum at $\theta = 0$ (black star). The inflection point in the CF is marked by a vertical green line.

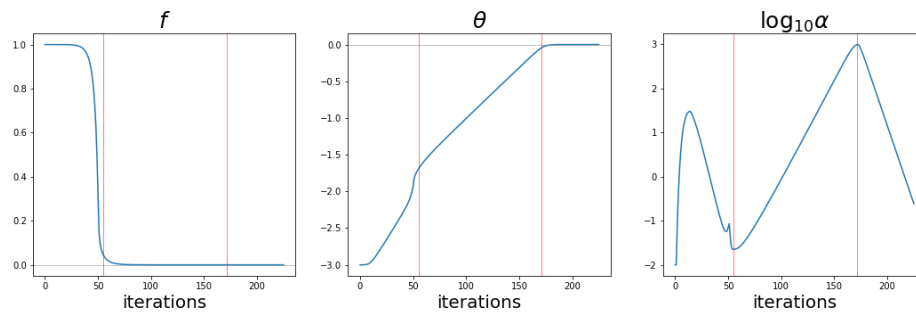


Figure 9: Comparative plots of the CF, θ , and α . Vertical lines are added to the plots to indicate turning points in the behavior of α .

in $\log \alpha$ between approximately *iterations* 13 and 50. Following that, θ is near -1.5 where the CF is relatively flat, and the updates still have to bring it to $\theta = 0$. One would expect α has to now increase in order to effect such change, and that is exactly what is seen in the rightmost plot of $\log \alpha$ between *iterations* = 55 and 171. Having reached *iterations* =171, θ is near zero, but not exactly. In order to make a "soft landing" at $\theta = 0$, α must start decreasing. Indeed, that is what the rightmost plot reveals from *iterations* = 171 onwards.

The quick changes of α when NeogradM is used on this CF highlight the importance of the responsiveness of an algorithm. It is not enough for an algorithm to slowly adapt to a changing CF landscape, as other algorithms do (cf. Duchi et al., 2011; Zeiler, 2012; Kingma and Ba, 2015). It must be able to make suitable adjustments almost immediately.

7.3 Beale’s Function

Beale’s function (Wikipedia, 2020) is used as a standard test for optimization algorithms, as it offers several challenging features in its CF landscape. It is defined as

$$f = (1.5 - \theta_1 + \theta_1\theta_2)^2 + (2.25 - \theta_1 + \theta_1\theta_2^2)^2 + (2.625 - \theta_1 + \theta_1\theta_2^3)^2.$$

It has a global minimum at $(\theta_1, \theta_2) = (3, 0.5)$. The initial condition used here is $(4, 3)$, from which is known the minimum is reachable. In Fig. 10 are comparison plots between Adam and NeogradM when applied to this CF. Once again, NeogradM reaches a much lower value than Adam in the $\log f$

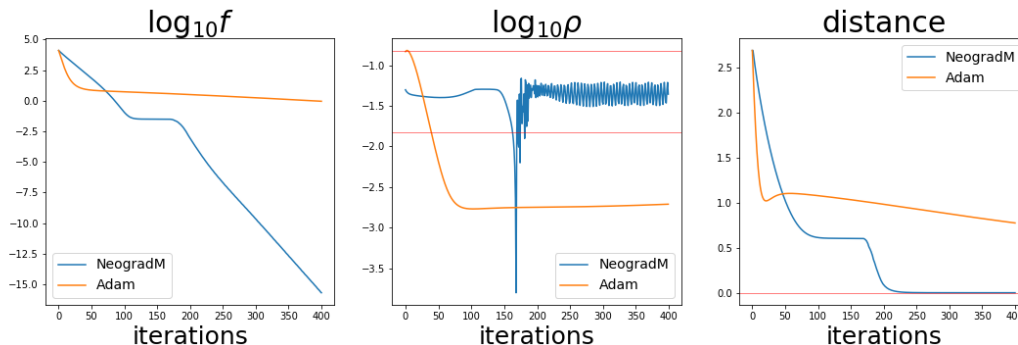


Figure 10: Comparison plots between NeogradM (blue) and Adam (orange). Of note is that NeogradM reaches a low CF value much more quickly (left plot), which mirrors its relatively high ρ values (center plot). NeogradM is thus able to close the distance to the minimum much more quickly than Adam (right plot).

plot; the exact number depends on how long the run is. Also, the plot of $\log \rho$ shows that Adam again naturally evolves into a situation where it produces very small ρ values, which as discussed are indicative of high UF (i.e., slow progress). The graph of $\log \rho$ due to NeogradM does a good job of staying within the red lines, except for a narrow spike to a low value. Recall that such overly small ρ values are merely inefficient, whereas overly large values are potentially problematic. This deviation seems to be a response to a very flat region in the CF profile. Finally, the right plot in the figure shows that NeogradM has reached its target after about 250 iterations, at which point Adam is still far from it.

It is illuminating to examine a plot of the updates of each algorithm as they move through the CF landscape. In Fig. 11 a red star indicates the starting point for the algorithms, and a black star the minimum. The path taken by NeogradM (the blue dots), takes a very direct route; it is nearly perpendicular to the contour lines. Recall that a pure GD algorithm would be perfectly perpendicular; the slight discrepancy is due to the momentum in NeogradM. In contrast, Adam takes a relatively oblique path toward the black star; it is clearly *not* perpendicular to the contour lines. As discussed in Sec. 2.1, Adam utilizes preferential weighting which adds significant weight to the null space term in the solution for $d\theta$ (cf. Eq. (2)), which are parallel to the contour lines. Thus, this plot is a visualization of that contribution.

7.4 Digit Recognition

Prior to this section, the CFs that were examined only had a 1 or 2 dimensional parameter space. In contrast, the current experiment uses a model where the dimensionality of θ is 2260. Specifically,

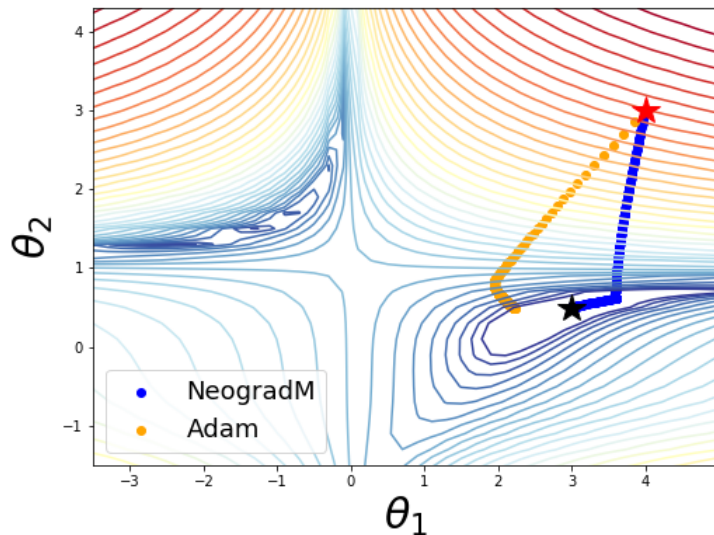


Figure 11: The red (black) star is the initial (final) point for NeogradM (blue dots) and Adam (orange dots). NeogradM clearly leads to a much better outcome. Note that the path due to Adam has a significant component parallel to the contour lines.

the model is that of a fully connected feed-forward neural network (NN) that is used to classify the digits 0-9. The digits data (Scikit-learn, 2020) were in the form of 8-by-8 images; there are 1437 labeled training images and 360 test images. The NN has one hidden layer, 64 input nodes, 30 hidden nodes, and 10 output nodes. No preprocessing was done on the input data, although it was one-hot encoded. A tanh activation function was used on the hidden layer, and a softmax on the final layer; a cross-entropy penalty CF was constructed between the output of the final layer and the training label. Also, the model had no regularization. Both Adam and NeogradM were used in training this NN model for a single run of 3500 iterations, resulting in Fig. 12 The most noticeable feature in the $\log f$ plot is that NeogradM leads to a significantly smaller value of the CF. Associated with that is the plot $\log \alpha$, which reveals the dramatic increase of α throughout the course of optimization. (In this figure the value of $\log \alpha$ for Adam is shown for reference.) This plot shows that α can and should be increased, in order to keep ρ in the target interval.

Next, in Fig. 13, a side-by-side comparison is made of $\log \rho$ for the two algorithms. As expected, NeogradM does a good job of keeping ρ in the target interval 4, whereas Adam falls far below it. This is similar to what was seen before with Adam. It also reveals that in this (somewhat) real application it's necessary to adjust α rather frequently, as is clear from the raggedness of the plot of $\log \rho$ for NeogradM.

In Fig. 14 a comparison is made between the sumd plots for the two algorithms. These plots have several interesting features, one of which is the rate of change of the updates. In this case the red vertical lines are drawn every 50 iterations, and they reveal that while NeogradM makes slow and steady progress, Adam instead makes initial rapid progress but then slows down suddenly. The vertical axes of these plots also show that $\|\theta\|$ changes by almost twice as much for NeogradM: 38.9

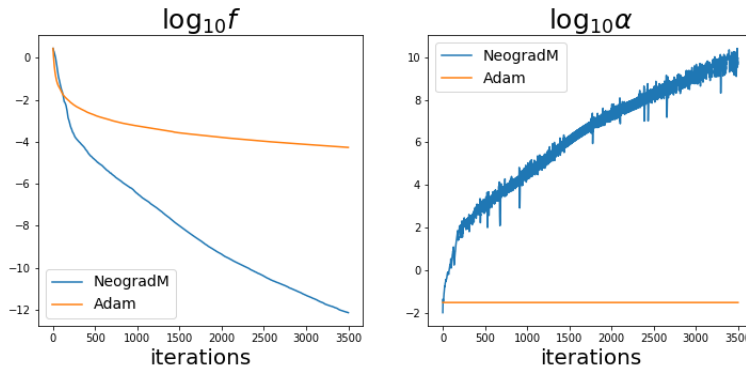


Figure 12: In the left plot, note the 8 order of magnitude improvement by NeogradM over Adam for $\log f$. In the right plot, observe how α increases to very large values as the optimization proceeds. (The value of α used in Adam is included for reference.)

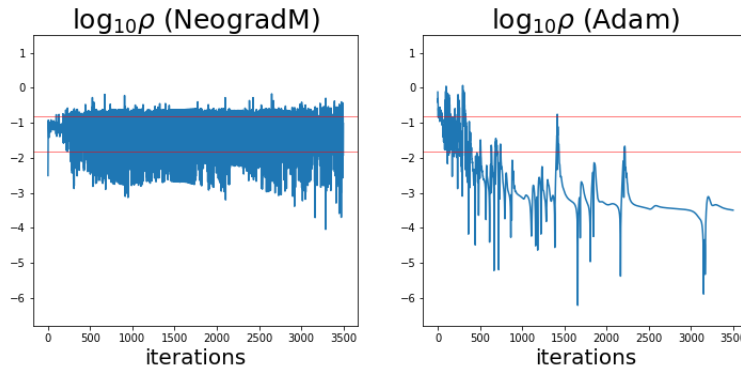


Figure 13: Illustration of $\log_{10} \rho$ for NeogradM (left) and Adam (right).

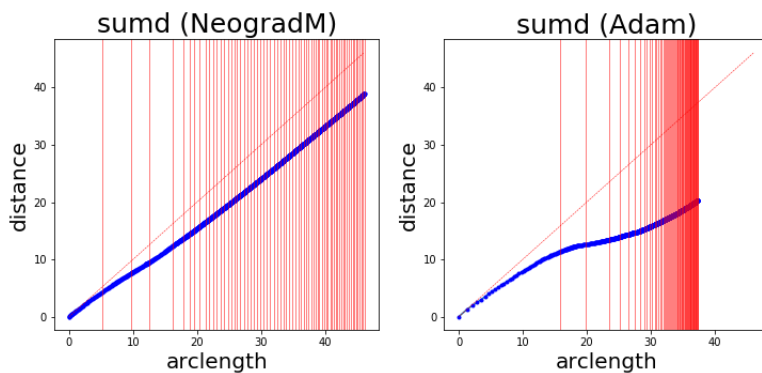


Figure 14: Illustration of $sumd$ for NeogradM (left) and Adam (right).

for NeogradM versus 20.3 for Adam. Also, the plot for Adam shows additional curvature that is not present for NeogradM. This indicates the updates for Adam are going in a different direction.

To further investigate the differences in the θ -paths from these two algorithms, three plots in Fig. 15 are presented. The left plot is a 2D comparison of the two parameter vectors, θ_{Adam} for

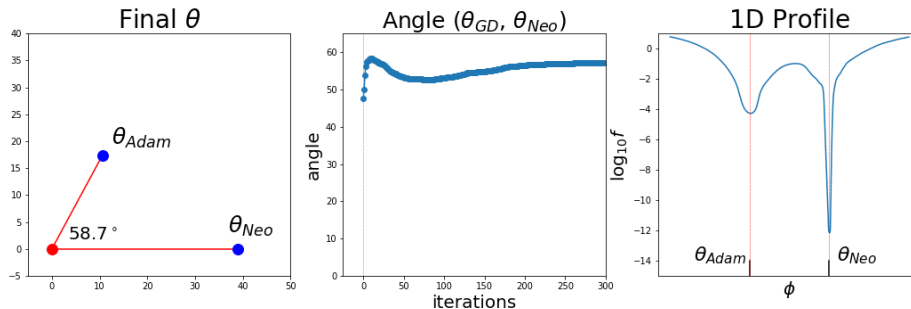


Figure 15: The left plot illustrates the differences in the magnitude and direction for the final parameter values for Adam and NeogradM (i.e., θ_{Adam} and θ_{Neo}); this indicates the algorithms found very different minima. The center plot shows this angular difference vs. iterations, and reveals that it largely appears after a single iteration. The right plot shows the profile of $\log f$ on a line connecting the two final θ values in θ -space; it shows they are well-separated basins of attraction, at least along this line.

Adam and θ_{Neo} for NeogradM. The angle between them is larger than might be expected, equalling over 58 degrees. To understand how this difference might result, a plot of the angle between θ_{Adam} and θ_{Neo} is given as a function of iterations. Somewhat surprisingly, almost all of the change in direction happens after the first iteration. This must reflect that Adam uses preferential weighting, and simply does not follow the direction of steepest descent. This was seen previously in the section on Beale’s function 7.3, where the presence of the different directions was notable. Finally, the third plot was included to make a simple comparison between the basins of attraction reached by each θ . (Keep in mind that this comparison is a select 1D plot, and the underlying dimensionality of the space is 2260.) The interpolating vector between the two θ s is defined as

$$\phi = (1 - s)\theta_{Adam} + s\theta_{Neo}.$$

In this plot the range of s is $[-1, 2]$. This plot shows the basins are distinct (at least along this one dimension). While it may seem that Adam has simply discovered a higher, slightly wider basin, it’s actually the case that it simply hasn’t followed the gradient of f down to lower values. Interestingly, if Adam were allowed to continue⁵ the optimization for an additional 3500 iterations, it would only have gone from $\log_{10} f = -4.27$ to -5.47 . However, if NeogradM had instead continued from where Adam left off at 3500 iterations, it would have gone from $\log_{10} f = -4.27$ to -9.28 . This shows it’s not that Adam somehow found a shallower basin, it’s that it wasn’t as effective in reaching a lower value in that basin.

The plots of this section have revealed that NeogradM outperforms Adam. In order to quantify this, the speedup is computed, as defined by the ratio t_2/t_1 , where t_1 (t_2) is the number of iterations

5. For this "continuation experiment", momentum variables were re-initialized to zero at the start of the run, for both Adam and NeogradM. The additional experiment of running Adam for 7000 iterations resulted in $\log f \approx -5.08$. Thus the restart slightly benefited Adam.

needed by Adam (NeogradM) to reach a specified CF value. (Another way to measure the performance increase is to compare CF values for a given iteration.) To reduce variation in the results due to the different initial θ s, 10 runs were made. In Fig. 16, three plots are shown of the results of this experiment Adam was run for 80000 iterations, while NeogradM was run until the limits of machine

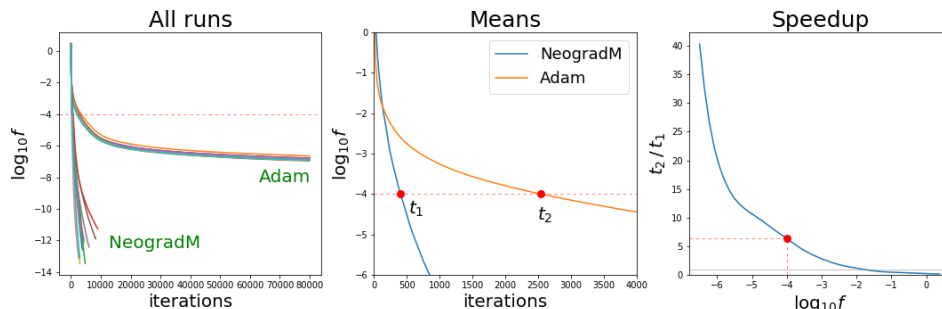


Figure 16: The left plot illustrates the 10 runs each for NeogradM and Adam; note the plateau in the upper grouping for Adam. The center plot uses the means from the 10 runs, and also illustrates how t_1 and t_2 are defined at the example value of $\log f = -4$ (cf. red dashed line). In the right plot, the speedup is plotted vs. $\log f$. Note its dramatic increase when Adam reaches its plateau. The red dashed lines indicate that at $\log f = -4$ the speedup is approximately 6.3.

precision caused it to stop. In the left plot, all runs are plotted. Although it seems like NeogradM has a higher variance (along the iteration axis), Adam actually has a higher variance for a given CF value because of its strong plateau. The center plot was obtained by computing the average number of iterations for a fixed CF value for each algorithm. It also gives a visual depiction of how the speedup is defined in this close-up view. Finally, in the right plot the speedup is computed for a larger range of the CF, and it reveals that in reaching these lower CF values, NeogradM is *much* faster than Adam. It is a reflection of the effective plateau in CF values produced by Adam, which seems to occur near $f \approx 10^{-7}$. Near the plateau, the speedup appears to become arbitrarily large. Note the dashed red lines in the right plot, which show that when trying to reach $\log f = -4$, the speedup by NeogradM over Adam is approximately 6.3.

To understand the cause of the variance in the left plot, the angles were computed for each pair of final θ values for the 10 runs for Adam, and the 10 runs for NeogradM. It was found that every such pair were nearly perpendicular⁶. This is a likely result of the extreme degeneracy of minima for NNs⁷

Finally, the analysis in this section has been when the CF was evaluated on the *training* data. Of course, in a real application one evaluates the resulting model on the testing data, to assess how well it generalizes. However, the goal here is to evaluate how well the algorithms *optimize*, not generalize. Nevertheless, to satisfy the curiosity of the reader, the results found indicated comparable

6. In a very high dimensional space, two randomly chosen vectors will likely be nearly perpendicular.
 7. The minima for the NN model will exhibit $n_h! \sim 10^{32}$ equivalent solutions, where n_h is the number of nodes in the hidden layer. This assumes there are no degeneracies in the solution space, such as when hyperplanes are (nearly) identical. It's easy to see that this results because when visualizing the connected nodes in the model, one can imagine transposing pairs of nodes in the hidden layer, with their connections remaining intact. Doing this would not change the model. Thus if all the pairs of weights attached to hidden nodes are distinct, there'll be $n_h!$ unique permutations (cf. p 277 in Goodfellow et al., 2016).

generalizability. Note that this may indicate that in order to generalize better the model needs to be refined, perhaps by adding some form of regularization.

7.5 2D Shell

While a simple polynomial function with gradual slopes is known to be easy fodder for a GD algorithm, CFs that have narrow wells are known to be much more challenging; they often lead to updates that oscillate about the minimum. The CF introduced here is meant as an extreme test in that regard, since it has a very narrow, curving well. This function is defined⁸ over $\theta = (\theta_1, \theta_2)$ as f :

$$\begin{aligned} f &= \sigma(z_1) + \sigma(z_2) + \zeta\theta_1 \\ z_1 &= s [(\theta_1/a)^2 + (\theta_2/b)^2 - r_1^2] \\ z_2 &= -s [(\theta_1/a)^2 + (\theta_2/b)^2 - r_2^2], \end{aligned}$$

where $r_1 = r + d$, $r_2 = r - d$, and σ is defined in Sec. 7.2; the remaining parameters are set to: $a = b = 1$, $r = s = 3$, $d = 0.2$, $\zeta = 0.01$. As with the sigmoid-well CF, this function is composed of two sigmoids as well. Here, $\sigma(z_1)$ creates a circular "well" of radius r_1 ; $\sigma(z_2)$ creates a circular "bump" of radius r_2 . When these two functions are added together, they create a narrow valley that follows a circular path, representing a degenerate minimum. To break this degeneracy, the term $\zeta\theta_1$ is added, creating a local minimum near $(-3, 0)$. Although this term tilts the entire CF landscape, this experiment is constrained so that updates should follow the local minimum of the circle. A view of a cross-section of this CF in Fig. 17 illustrates the effect of this term.

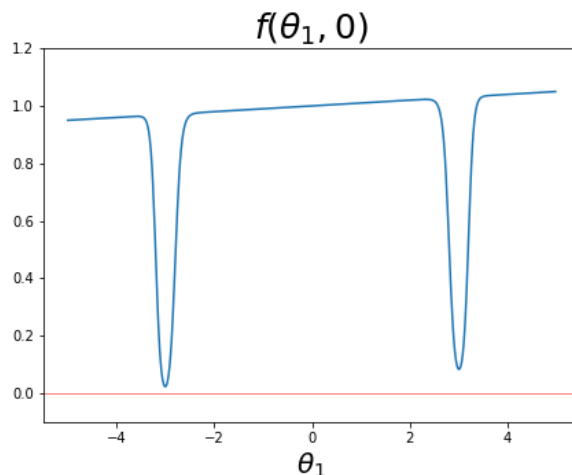


Figure 17: Cross-section of *2Dshell* at $\theta_2 = 0$.

In previous sections the emphasis had been on plots of the CF vs. *iterations*. Here it is easier to form a comparison by examining two plots: $\log \rho$ vs *iterations*, and an overhead visual of the path of updates in the (θ_1, θ_2) plane. In the figures, the two white stars mark the start and end points,

8. This function can be generalized to higher dimensions. However, 2-dimensions was enough to create a challenging CF. In higher dimensions, the updates stay in one plane, so it ends up acting like the 2D version anyway.

with the start point being $\theta = (4, 1)$ and the end point near $\theta = (-3, 0)$. The ideal behavior of the algorithm is to move slightly left, drop down into the local well, and then follow it counter-clockwise until it reaches the local minimum near $(-3, 0)$. The best algorithm will be judged by its ability to follow this path in a stable and efficient manner, and also to get as close as possible to the end point. The $\log \rho$ plot will be used to judge its stability and efficiency. For all of the following figures, the number of iterations was 1200, and the learning rate was chosen to show (near) optimal behavior of the algorithms.

With the Adam algorithm, $\alpha = 0.15$ was used. Immediately noticeable in Fig. 18 is the erratic graph of $\log \rho$, which shows a limited amount of stability. When a smaller α was used, its stability

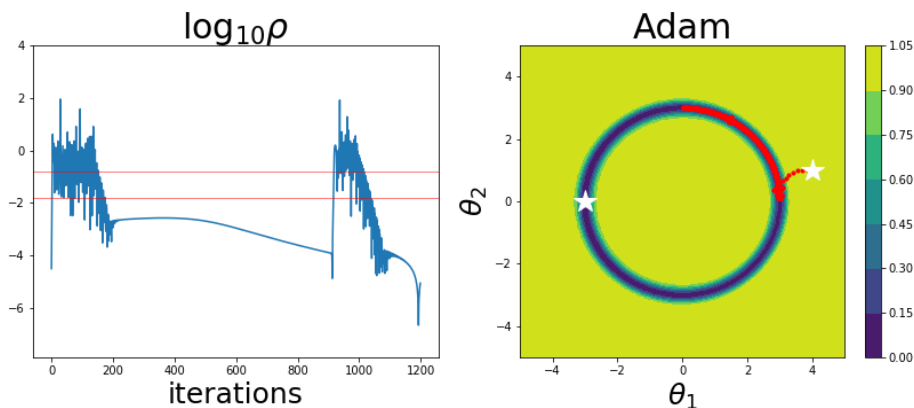


Figure 18: In the left plot, $\log \rho$ strays significantly from the interval set by the red lines, indicating either unstable behavior (i.e., $\rho > \rho_{max}$) or inefficient updates ($\rho < \rho_{min}$). The right plot reveals the updates have difficulty when first entering the well, which is reflected in the left plot.

improved, but at the expense of progress toward the minimum. In comparison to RMS Prop (figure available at Zimmer, 2020b), it clearly does better. Actually, the general trend was that any algorithm that utilized momentum did much better than its momentum-free version. Apparently, when faced with a narrow well, the ability of momentum to average out mistakes is more important than just making smaller mistakes.

The results in Fig. 19 from NeogradM showed a significant contrast First, it was very stable, as ρ stayed within its target interval to a large degree. The updates also took it closer to the minimum near $(-3, 0)$. The Neograd algorithm (i.e., the version of NeogradM without momentum), didn't do nearly as well (cf. results on Zimmer, 2020b). As mentioned earlier, the role of momentum is apparently very important in dealing with narrow valleys.

The algorithm NeogradM_dbl was also used for updates on this CF, as shown in Fig. 20. The $\log \rho$ plot is much improved, in that it is better at respecting the boundaries of $(\log \rho_{min}, \log \rho_{max})$. Also, the path of the updates ends up close to the target of the white star on the left. From these two plots, this algorithm is visibly better than all the others. This was to be expected, as it is basically NeogradM except with a double computation of the CF. In the $\log \rho$ plots in Figs. 19 and 20, one of the first values is large, and above ρ_{max} . This is due to the updates taking θ through the sudden drop as it enters the narrow valley. This issue will be addressed elsewhere Zimmer (2020a).

In Fig. 21 is shown a comparison between the dotp and sumd diagnostics for Adam. The most notable aspects displayed here are the reversals in direction that are apparent in both plots. Recall

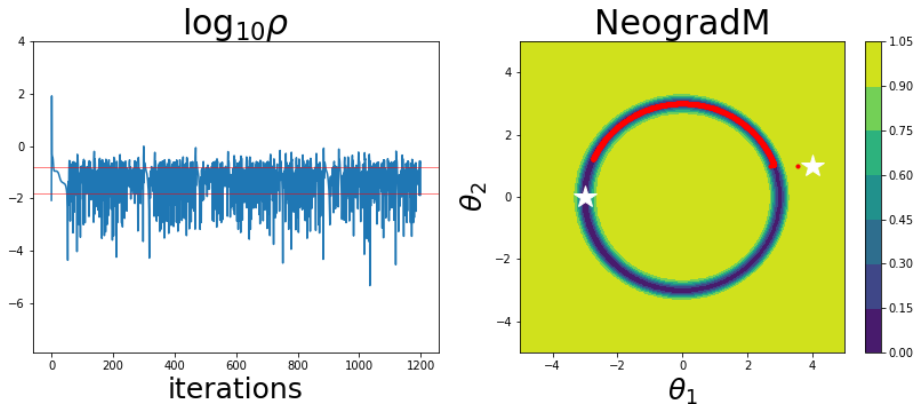


Figure 19: In the left plot, ρ stays more consistently within or below the target interval. The only exception is at the very beginning, when the updates of θ take it through a steep drop into the well. The right plot reveals an overall smoother trajectory than that for Adam.

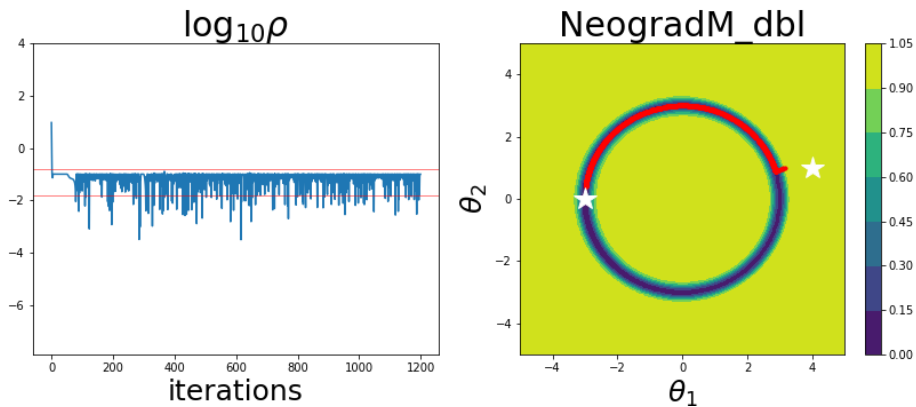


Figure 20: The left and right plots are similar to those in Fig. 19 except that here the updates are smoother and with better results. This is to be expected since the update of θ is done twice for each iteration.

that when successive $d\theta$ values are in opposite direction, $\text{dotp} \approx -1$, and the overall distance change is approximately zero. This is exactly what's indicated in these two plots: the two regions in dotp with negative values correspond to the two regions of the sumd plot where the slope is approximately zero. (The correspondence can be determined after realizing the red vertical lines in the sumd plot are drawn every 50 iterations.) Another reason for the slope of the sumd plot to be near zero is when $d\theta$ is perpendicular to $(\theta - \theta_0)$; this actually occurs at the beginning of the run, soon after the updates take it into the well. Whenever the slope of the sumd is near 45 degrees, $d\theta$ and $(\theta - \theta_0)$ point in the same direction. An inspection of Fig. 18 reveals that such could have been the case for the entire latter half of the sumd plot, were it not for the brief interruption where dotp was negative (as already discussed).

In Fig. 22 the same comparison plot is shown for NeogradM_dbl. Here, dotp is almost exactly 1.0, for the whole course of the optimization, which indicates the process was very stable with no

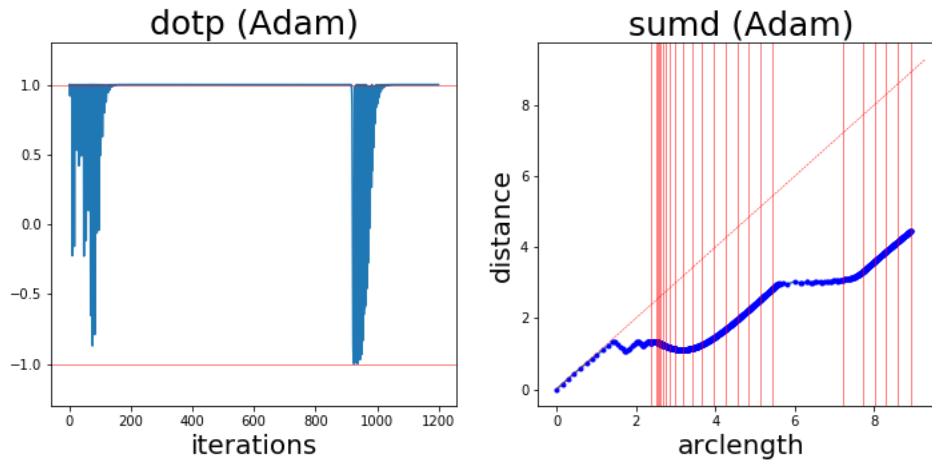


Figure 21: The *dotp* diagnostic in the left plot reveals unstable behavior early and late in the optimization. That behavior is mirrored in the *sumd* plot on the right, which shows a lack of progress in the *distance* at the corresponding number of iterations. Vertical lines in the *sumd* plot are drawn every 50 iterations.

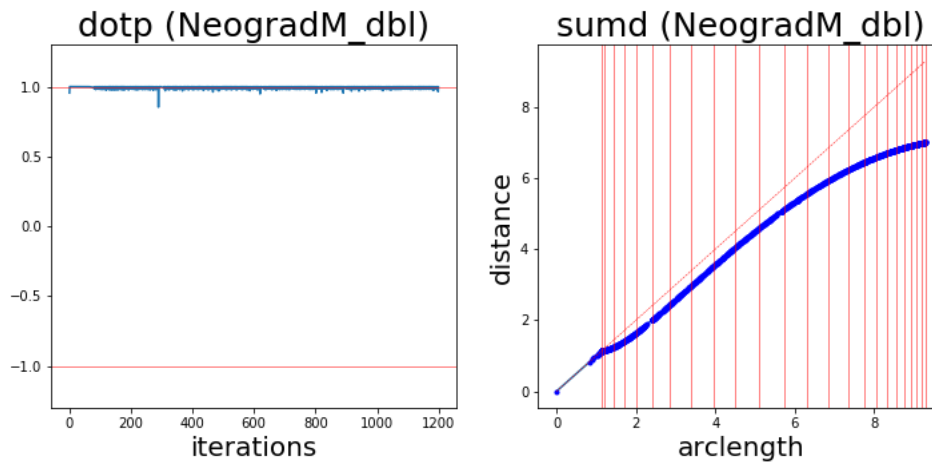


Figure 22: In contrast to the previous plots for Adam, *dotp* reveals no unstable behavior. This is mirrored by the *sumd* plot, which shows smooth progress throughout the run. Vertical lines in the *sumd* plot are drawn every 50 iterations.

reversals. Also, the vertical red lines in the *sumd* plot occur very regularly, which indicates the updates are made at a somewhat constant size. Toward the end of the run, the *sumd* graph has a slope that's veering away from 45 degrees toward zero. As already explained, a small slope occurs when the updates to θ are becoming perpendicular to $(\theta - \theta_0)$. Since θ_0 was $(4, 1)$, this won't happen exactly when θ is at the minimum near $(-3, 0)$, but it is close.

7.6 Manual Adjustment of α

In some cases the user of an optimization algorithm may wish to adjust α manually, based on the value of ρ . For example, in Fig. 7, the value of ρ is quite low after about iteration 100, and its $\log \rho$ value would need to be shifted upward by about $\log_{10} 50 \approx 1.7$ to be comparable to the $\log \rho$ value for NeogradM. With that in mind, an experiment is done here, in which at iteration 100, α is increased by a factor of 50 for Adam. Thus, before iteration 100, $\alpha = 0.15$, and afterwards $\alpha = 0.15(50) = 7.5$. (The reason why the same factor can be used for α and ρ is that for small ρ they're proportional, as indicated by Eq. (9).) The result of this experiment is shown in Fig. 23. First,

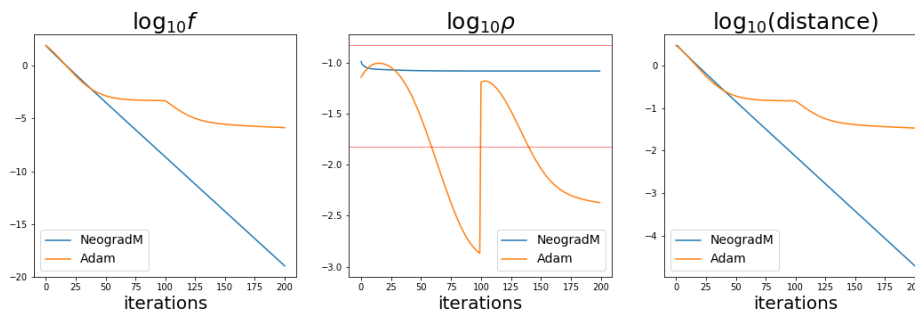


Figure 23: An illustration of the effect of a manual adjustment of α from 0.15 to 7.5 on Adam, at the 100th iteration. This is done for the quartic CF, and the graph is otherwise the same as for Fig. 7. Because ρ is small, when α is increased by a factor of 50, ρ also increases (approximately) by the same factor.

the plot of $\log \rho$ shows that the factor of 50 increase in α led to a factor of approximately 50 increase in ρ , as expected. Second, what all three plots reveal is that the effect is *temporary*. Whatever the dynamics of the Adam algorithm are, they seem to invariably lead to a small ρ value. Third, this experiment reveals that it is indeed possible to make manual adjustments of α using information from the ρ diagnostic, in order to achieve better performance from the optimization. However, this is what is done automatically by Neograd with Eq. (9), the adaptation formula for α .

8. Final Remarks

The motivation that led to this paper was to better understand and control the learning rate (α) so that it could be more efficiently utilized in the gradient descent algorithm. The solution introduced herein was based on the concept of *update fidelity* and the ρ diagnostic; other diagnostics played a supporting role. Together they provide a window into the behavior of GD-like algorithms in arbitrarily high dimensional spaces.

In several basic examples, it was shown that α and ρ were connected by a relatively simple relationship, and that it was possible to easily solve for α in terms of ρ , if only approximately. From this the *constant ρ ansatz* was formulated, in which it was postulated that an ideal algorithm would adjust α so as to keep ρ at a constant, acceptable value. A comparison between ρ and the cutoff of 0.05 for p-values in statistics was made, in which both were viewed as *quality control* parameters.

In order to be able to handle an arbitrarily complex CF, this approach was generalized, and an *adaptation formula* for α was derived (see Eq. (9)). Using this formula as a basis, the Neograd family of algorithms were defined, as well as hybrid algorithms between those and the GD family of

algorithms. A number of numerical experiments were performed, each with the intent to illustrate some feature or make some comparison. An exhaustive comparison between the algorithms was *not* performed; instead the focus was on Adam vs. NeogradM. The most general takeaway from these experiments was that NeogradM vastly outperforms Adam: it reaches lower CF values in a shorter time and does so with more stable updates. While Adam generally leads to a CF vs. *iterations* profile that at first quickly decreases and then flattens out (i.e., "plateaus"), NeogradM would instead quickly decrease and keep on doing so. In fact, optimization runs done with NeogradM were simply run until the limits of machine precision were felt; no other stopping condition was needed. In addition, there is a time benefit to using NeogradM, as it automatically adjusts α . In contrast, Adam requires several costly trial runs beforehand. As a general characterization, algorithms from the GD family might be called *uncontrolled* since they do not monitor or attempt to control the algorithm using something like the ρ diagnostic.

Care must be taken in evaluating this optimization algorithm in the context of ML applications. In such a setting the comparison is usually based on the ability of the algorithm to *generalize*. However, optimization is not the same as generalization; the latter normally includes regularization as well. While the NeogradM algorithm is meant as a pure optimization algorithm, it is argued here that Adam is a mix between optimization and regularization. This is stated because built into it is an early stopping mechanism, which arises naturally and in an uncontrolled way by the appearance of its *plateau*. Also, since it's the case that NeogradM is able to lower the CF to much lower values than current algorithms, it may force the modeler to think more carefully about regularization in order to more fully exploit the improved minimization.

As the Neograd family has been introduced, it is intended to be used in a batch processing mode when used in an ML context. It *can* be applied in a mini-batch mode (or as "SGD"), but there will be differences. The approach of SGD is somewhat different, as the CF changes with each mini-batch (since the data changes, and the data defines the CF). An investigation by the author may be made elsewhere. Also, an analysis and some extensions of the Neograd algorithms will be made elsewhere Zimmer (2020a).

Acknowledgement

The author thanks Sebastian J. Wetzel for his suggestions on improving the manuscript.

Appendix A: In Situ Row Space Solution for $Ax = b$

This appendix presents a simpler, more intuitive derivation of the *row space in situ* method Zimmer (2020c) used for solving a system of linear equations. It is notable in that it is formulated solely in terms of the row space of the coefficient matrix, never requiring gaussian elimination. In addition, it permits an online formulation.

The method begins with the realization that it's possible to effect linear operations on the rows of a matrix by left multiplying it with suitable matrices. By extension, it's possible to effect a Gram-Schmidt orthonormalization of the rows of a matrix by repeated left-multiplication using suitable matrices. In the case at hand, the system of linear equations is described by the matrix equation $Ax = b$, where A is the m -by- n coefficient matrix, x is the n -dimensional vector of unknowns, and b is an m -dim vector. For this appendix, all entries are assumed to be real. Also, take $m \leq n$, and assume A has full row rank (the general case is treated in Zimmer, 2020c). Define the product of

m-by-m matrices M_i with $i = 1, \dots, t$ to be $M = M_t \dots M_1$, which are chosen to orthonormalize the rows of A . Multiplying both sides of $Ax = b$ by M yields $A'x = b'$, where $A' = MA$ and $b' = Mb$. Note that the rows of A' form an orthonormal set.

At this point the reader should pause and realize that $x \in R^n$ and that there is an m-dimensional orthonormal basis available via the rows of A' . It follows that x may be expressed as

$$x = \alpha_1 v_1^T + \alpha_2 v_2^T + \dots + \alpha_m v_m^T + \beta_1 w_1 + \dots + \beta_{n-m} w_{n-m},$$

where the α_i and β_j are suitable coefficients, v_i are the rows of A' , w_j represents a basis for the null space, $i = 1, \dots, m$, and $j = 1, \dots, n - m$. This solution is more simply expressed using A'

$$x = (A')^T \alpha + x_{null},$$

where $\alpha = (\alpha_1, \dots, \alpha_m)^T$, and x_{null} represents the previous sum $\sum \beta_j w_j$. (Another way to express x_{null} is Py , where P is the null space projection matrix $(1 - A'^T A')$ and y is an arbitrary n -dimensional vector.) After substituting this expression into $A'x = b'$, it's clear that $\alpha = b'$, and the solution may be written as

$$x = (A')^T b' + x_{null}.$$

Finally, observe that since the particular solution is built from the row space (and not the null space) of A , it is a *minimum norm* solution. This also follows from a characterization of its corresponding generalized inverse (see Zimmer, 2020c).

In the context of gradient descent (i.e., Eq. 1), A is a matrix with a single row, with entries corresponding to the gradient of a function f (assumed to have n components). Thus, A is 1-by- n , x is n -by-1, and b is 1-by-1. To orthonormalize $A = \nabla f$, it's only necessary to normalize it; hence $M = 1/\|\nabla f\|$ is a scalar. It follows immediately that the solution is

$$x = \frac{b}{\|\nabla f\|^2} (\nabla f)^T + x_{null}.$$

By identifying $x = d\theta$ and $b = -|\delta f|$, Eq. 2 results.

Finally, this approach yields the incidental result of demonstrating that the gradient of a function points in the direction of its maximal increase. Up until now, δf was fixed, and $d\theta$ was solved for. However, one can instead let δf vary, fix $\|d\theta\|$, and set

$$d\theta = d\theta_{min} + d\theta_{null},$$

where $d\theta_{min}$ is parallel to ∇f , $d\theta_{null}$ is perpendicular to ∇f , and thus

$$\|d\theta\|^2 = \|d\theta_{min}\|^2 + \|d\theta_{null}\|^2.$$

Given this, it's immediately clear that maximizing $\|\delta f\| = \|\nabla f \cdot d\theta\|$ means minimizing $\|d\theta_{null}\|$; thus, $d\theta_{null} = 0$ and $d\theta$ is parallel to ∇f . If one is careful with the \pm signs, it can be seen that the gradient points in the direction leading to the maximal *increase* of f , a result otherwise known from calculus.

Appendix B: Another Definition of ρ

Given Fig. 1, another equally reasonable definition for a metric to quantify the UF is

$$\rho_2 = \left| \frac{f_{new} - f_{est}}{f_{new} - f_{old}} \right|.$$

Note that when $\rho_2 \rightarrow 0$, the two metrics become equal. Using the same definitions of A and B from Sec. 6.1, it can be rewritten as

$$\rho_2 = \left| \frac{\alpha A}{\alpha A + B} \right|.$$

This absolute value equation may be inverted to yield two solutions for α

$$\alpha_{\pm} = \frac{B}{A} \left(\frac{\pm \rho_2}{1 \mp \rho_2} \right).$$

At any time, only one is greater than 0, and that will be the one selected. Hence Eq. (9) would be replaced by $\alpha = \max(\alpha_+, \alpha_-)$. Although the equations are similar, the behavior of ρ_2 isn't as convenient as with ρ . The denominator leads to a divergence when $f_{new} = f_{old}$, which can happen in the vicinity of a minimum, for example. Also, this new form of the adaptation formula involves two cases (α_{\pm}), which isn't as simple as Eq. (9).

For completeness, also observe that the sign of α_{\pm} changes according to whether f is concave up/down. Also, the signs in Table 2 assume $\rho_2 < 1$, since only that range would be used in the

Table 2: Signs of various quantities depending on the concavity of f . In all cases, assume $\rho_2 < 1$.

	A	B	α_+	α_-
concave up	+	-	-	+
concave down	-	-	+	-

algorithms; for $\rho_2 > 1$ the table changes.

References

- A. Cauchy. Méthode générale pour la résolution des systèmes d'équations simultanées. *C. R. Acad. Sci. Paris*, 25:536–538, 1847.
- A.-A. Cournot and T.H. Martin. Galileo Galilei. URL en.wikiquote.org/wiki/Galileo_Galilei.
- J. Duchi, E. Hazan, and Y. Singer. Adaptive subgradient methods for online learning and stochastic optimization. *Journal of Machine Learning Research (JMLR)*, 12:2121–2159, 2011.
- I. Goodfellow, Y. Bengio, and A. Courville. *Deep Learning*. The MIT Press, 2016.
- D.P. Kingma and J.L. Ba. Adam: A method for stochastic optimization. In *International Conference on Learning Representations (ICLR)*, 2015.

- F.-F. Li et al. Cs231n: Convolutional neural networks for visual recognition, 2020. URL <http://cs231n.stanford.edu>.
- Y. Nesterov. A method for unconstrained convex minimization problem with the rate of convergence $O(1/k^2)$. *Soviet Mathematics Doklady*, 27:372–376, 1983.
- R. Pascanu, T. Mikolov, and Y. Bengio. On the difficulty of training neural networks. In *International Conference on Machine Learning (ICML)*, 2013.
- B.T. Polyak. Some methods of speeding up the convergence of iteration methods. *USSR Computational Mathematics and Mathematical Physics*, 4(5):1–17, 1964.
- W.H. Press, S.A. Teukolsky, W.T. Vetterling, and B.P. Flannery. *Numerical Recipes, The Art of Scientific Computing*. Cambridge University Press, 3rd edition, 2007.
- S. Ruder. An overview of gradient descent optimization algorithms. *arXiv preprint*, arXiv:1609.04747, 2017.
- Scikit-learn. Digits dataset, 2020. URL https://scikit-learn.org/stable/modules/generated/sklearn.datasets.load_digits.html.
- W. Shakespeare. *Macbeth*.
- T. Tieleman and G. Hinton. Lecture 6.5 - RMSProp, Coursera: Neural networks for machine learning. Technical report, 2012.
- Wikipedia. Test functions for optimization, 2020. URL http://en.wikipedia.org/wiki/Test_functions_for_optimization.
- M.D. Zeiler. Adadelata: an adaptive learning rate method. *arXiv preprint*, arXiv:1212.5701, 2012.
- M.F. Zimmer. Document in preparation., 2020a.
- M.F. Zimmer. Github repository, 2020b. URL www.github.com/mfzimmer.
- M.F. Zimmer. Two direct solvers for a system of linear equations. *arXiv preprint*, arXiv:1611.06633, 2020c.